# Shuttle-Cargo fusion molecules of transport peptides and the hD 2/3 receptor antagonist fallypride : a feasible approach to preserve ligand-receptor binding?

Wängler, Carmen; Chowdhury, Shafinaz; Höfner, Georg; Djurova, Petia; Purisima, Enricho O.; Bartenstein, Peter; Wängler, Björn; Fricker, Gert; Wanner, Klaus T.; Schirrmacher, Ralf



**Publisher's version / Version de l'éditeur:**
https://doi.org/10.1021/jm5004123
*Journal of Medicinal Chemistry, 57, 10, pp. 4368-4381, 2014-04-30*

Journal of Medicinal Chemistry

Article

pubs.acs.org/jmc

# Shuttle–Cargo Fusion Molecules of Transport Peptides and the $hD_{2/3}$ Receptor Antagonist Fallypride: A Feasible Approach To Preserve Ligand–Receptor Binding?

Carmen Wängler,[*,†,‡,§] Shafinaz Chowdhury,[∥] Georg Höfner,[⊥] Petia Djurova,[#] Enrico O. Purisima,[▽] Peter Bartenstein,[§] Björn Wängler,[○] Gert Fricker,[#] Klaus T. Wanner,[⊥] and Ralf Schirrmacher[†]

[†]McConnell Brain Imaging Centre, Montreal Neurological Institute, McGill University, Montreal H3A 2B4, Canada

[‡]Biomedical Chemistry, Department of Clinical Radiology and Nuclear Medicine, Medical Faculty Mannheim of Heidelberg University, Mannheim 68167, Germany

[§]Department of Nuclear Medicine, University Hospital Munich, Ludwig-Maximilians-University Munich, Munich 81377, Germany

[∥]Lady Davis Institute, Jewish General Hospital, McGill University, Montreal H3T 1E2, Canada

[⊥]Pharmaceutical Chemistry, Ludwig-Maximilians-University Munich, Munich 81377, Germany

[#]Institute of Pharmacy and Molecular Biotechnology, University of Heidelberg, Heidelberg 69120, Germany

[▽]National Research Council of Canada, Montreal H4P 2R2, Canada

[○]Molecular Imaging and Radiochemistry, Department of Clinical Radiology and Nuclear Medicine, Medical Faculty Mannheim of Heidelberg University, Mannheim 68167, Germany

*S* *Supporting Information*

**ABSTRACT:** To determine if the conjugation of a small receptor ligand to a peptidic carrier to potentially facilitate transport across the blood–brain barrier (BBB) by "molecular Trojan horse" transcytosis is feasible, we synthesized several transport peptide–fallypride fusion molecules as model systems and determined their binding affinities to the $hD_2$ receptor. Although they were affected by conjugation, the binding affinities were found to be still in the nanomolar range (between 1.5 and 64.2 nM). In addition, homology modeling of the receptor and docking studies for the most potent compounds were performed, elucidating the binding modes of the fusion molecules and the structure elements contributing to the observed high receptor binding. Furthermore, no interaction between the hybrid compounds and P-gp, the main excretory transporter of the BBB, was found. From these results, it can be inferred that the approach to deliver small neuroreceptor ligands across the BBB by transport peptide carriers is feasible.

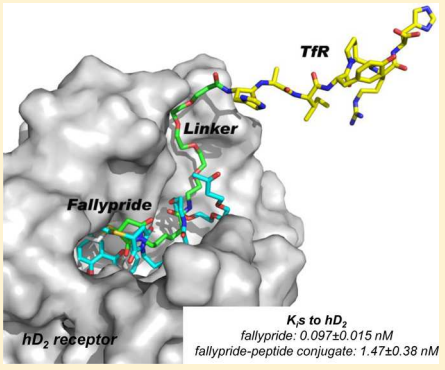


## INTRODUCTION

Functional diagnosis and treatment of diseases of the central nervous system (CNS) are still limited by the blood–brain barrier (BBB), a combination of endothelial tight junctions and active drug transporters, preventing the accumulation of hydrophilic as well as lipophilic drugs in the brain parenchyma (Figure 1A,B).[1] While exercising the very important physiological role of protecting the CNS against potentially toxic compounds, it limits diagnostic and therapeutic opportunities in the case of disease. Thus, many efforts have been made within recent decades to overcome this barrier.[2−6] Most strategies use the so-called molecular Trojan horse approach, which makes use of drug conjugates combining a shuttle (a substance that is able to cross the BBB by transcytosis; Figure 1C,D) and a cargo (a diagnostic or therapeutic drug that is intended to be taken up into the CNS and is not able to cross the BBB on its own; Figure 1E).

Following this approach, different substance classes have been used as shuttle vectors. So far, mostly large bioactive molecules such as antibodies directed against the transferrin receptor (TfR) (TfRmAbs, such as OX26) or the insulin receptor (IRmAbs), other proteins such as melanotransferrin, receptor associated protein, and CRM197 (a nontoxic mutant of diphtheria toxin), or liposomes functionalized with peptides or proteins have been applied.[2,3,7−9] However, although exhibiting a highly specific accumulation in the target, the use of large molecules as drug carriers is unfavorable with regard to their drug pharmacokinetics, clearance, immunogenicity, and bioavailability. Furthermore, a fusion molecule composed of a large carrier and a small neuroreceptor-binding cargo is commonly regarded as being unlikely to exhibit a preserved affinity of the ligand to its intended target.

**Received:** March 16, 2014
**Published:** April 30, 2014

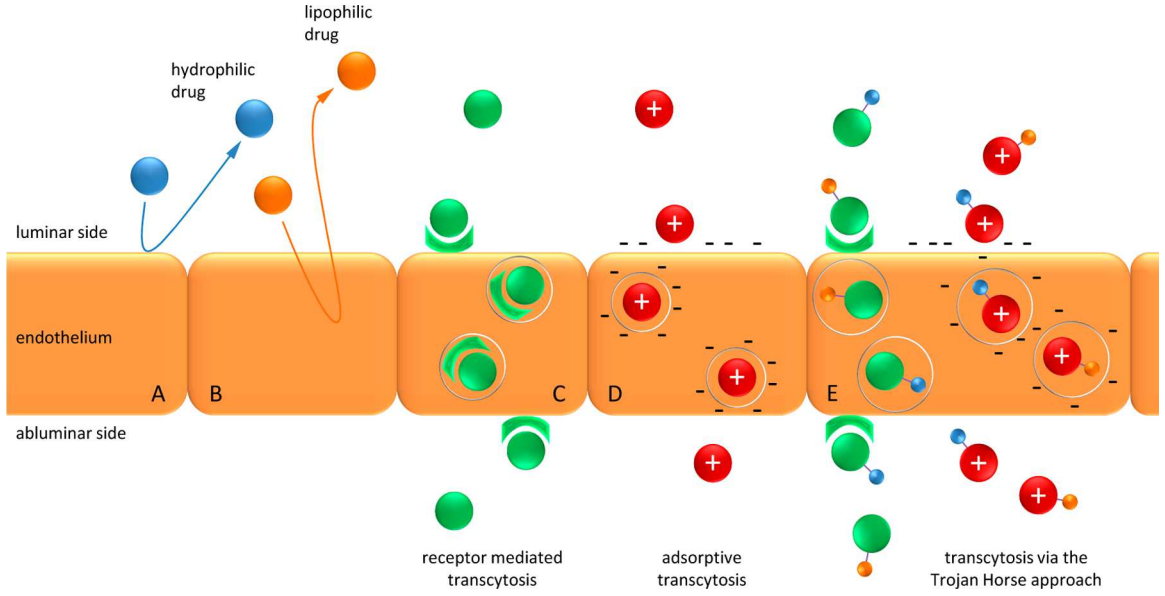


**Figure 1.** Schematic depiction of the different mechanisms of BBB function and transcytosis: hydrophilic drugs cannot enter the endothelium (A), some lipophilic drugs can enter the endothelium but get externalized by active drug transport (B), BBB crossing of receptor-binding substances such as transferrin and insulin by receptor-mediated transcytosis (C), unspecific BBB crossing of positively charged substances by adsorptive transcytosis (D), and specific or nonspecific BBB crossing of hydrophilic (blue) or lipophilic (orange) drugs using the molecular Trojan horse approach by receptor-mediated or adsorptive transcytosis (E).

Therefore, the use of smaller peptides as shuttles across the BBB has been proposed. Peptides that are, in principle, applicable for cargo delivery to the brain are neuropeptides that are transported across the BBB by endogenous transporters (Figure 1C), such as transferrin receptor binding peptides (transported via the TfR),[10] neurotensin (transported via neurotensin receptors NTS1, NTS2, and NTS3),[11,12] cholecystokinin (transported via cholecystokinin receptors CCKR1 and CCKR2),[12,13] neuropeptide Y (transported mostly via receptors Y1, Y2, Y4, and Y5),[12,14] and Substance P (transported via the neurokinin receptor)[15] as well as AngioPep-2 and other peptide derivatives that are transported via the low-density lipoprotein related receptor, LRP1.[16−20] Furthermore, cell-penetrating peptides such as SynB,[21,22] Penetratin,[23,24] vasoactive intestinal peptide (VIP),[25] Transportan,[26] and TAT[27−30] derivatives as well as polyarginines[31] that have been shown to enter the brain via different transduction mechanisms[32,33] (Figure 1D) are also promising peptidic carriers for transporting small molecule drugs across the BBB.

The use of peptides is favorable because they are highly potent substances that display a low immunogenicity and molecular weight, resulting in fast pharmacokinetics and background clearance. Furthermore, they are easily accessible by chemical synthesis and can be site-specifically derivatized with a cargo drug. All of this makes peptides promising carriers for small drug molecules that can have a higher chance of preserving the biological activity of the drug compared to that when using larger shuttles.

A successful fusion molecule consisting of a peptide and a small drug thus has to fulfill the following requirements: (i) the shuttle has to target a transcytosis receptor system with high affinity or has to be able to pass the BBB by a passive mechanism, (ii) the ability of the shuttle to cross the BBB has to be maintained after conjugation of the cargo drug, and (iii) the cargo drug has to preserve its biological activity upon conjugation to the shuttle.

Because a small drug molecule is structurally altered significantly by conjugation to a peptide, it is conceivable that such a conjugation would most likely result in a fusion molecule of diminished or even eliminated binding affinity of the ligand to its target receptor. Similar effects of drastically decreased binding properties (up to 6 orders of magnitude) upon conjugation of large constructs have been shown exemplarily on the biotin−streptavidin system recently.[34,35]

Thus, we intended to investigate if the conjugation of a small neuroreceptor-affine drug to a carrier peptide can, in principle, result in a hybrid compound that is potentially able to transport the small molecule while at the same time preserving its affinity to the neuroreceptor. We therefore synthesized a palette of fusion drugs, each consisting of a peptide carrier and a derivative of the $hD_{2/3}$ receptor-binding drug fallypride in order to test the feasibility of this approach.

Fallypride was used as the model neuroreceptor-binding drug because is used in its $^{18}F$-labeled form in human in vivo $hD_{2/3}$ receptor imaging with positron emission tomography (PET),[36−38] thus making it a well-studied ligand system. In addition, for its counterpart, the $hD_2$ receptor system, an in vitro receptor binding assay is available to study the $hD_2$ receptor affinities of the developed hybrid molecules.

For these fallypride and transport peptide conjugates, we determined the binding affinities to the $hD_2$ receptor in vitro and found that although a decrease in $hD_2$ receptor affinity is observed upon conjugation of fallypride to the peptides, the remaining binding affinity is still surprisingly high and remains in the nanomolar range. In order to explain and corroborate these experimental findings, we conducted homology modeling of the $hD_2$ receptor, starting from the $hD_3$ receptor as the template, and performed docking studies of the two most potent hybrid compounds, elucidating the contribution of different structure elements to receptor binding. We also


dx.doi.org/10.1021/jm5004123 | J. Med. Chem. 2014, 57, 4368−4381

conjugated structural motifs to some of the synthesized hybrid molecules, allowing for radiolabeling with $^{68}$Ga and $^{18}$F and future in vivo PET imaging of $hD_{2/3}$ receptors. Furthermore, the interaction between the most promising hybrid compounds and the main excretory transporter of the BBB, P-glycoprotein, was studied.

## RESULTS AND DISCUSSION

As peptidic carriers, different peptides with the potential to enter the brain parenchyma by receptor-mediated transcytosis (two different transferrin receptor binding peptides as well as AngioPep-2) or adsorptive transcytosis (TAT, $TAT_{49-57}$, transportan, penetratin, and the nuclear localization sequence of human NF-κB) were chosen as model peptides. They strongly vary in length, structure, polarity, and geometry. This structural diversity was intended to elucidate possible influences of the peptide architecture on the $hD_2$ receptor affinity of the fallypride moiety in the resulting fusion drugs. Furthermore, the influence of linker structures and lengths between the peptide carrier and the receptor ligand was systematically evaluated.

**Synthesis of Thio-fallypride (FP-T, 1).** The first step in the stable conjugation of fallypride to different peptidic carriers was the synthesis of a fallypride derivative containing a functional group in the terminal nonpharmacophoric position of the alkyl chain for peptide coupling. For this purpose, thiol-functionalization of fallypride was chosen because peptides can be easily modified with maleimides and subsequently reacted efficiently and site-specifically with thiol-bearing synthons, yielding a defined fusion molecule via simple and efficient click chemistry.

The first attempts to obtain a thiol-functionalized fallypride molecule were made by implementing protected thiol-bearing synthons in the fallypride scaffold synthesis, resulting, however, only in the formation of byproducts. Hence, it was intended that the thiol functionality would be introduced by reacting tosyl-fallypride (FP-Tos)[39] with *S*-acetyl-thioethanolamine, 1,2-ethanedithiol, or 2,2′-dithiobis(ethylamine) dihydrochloride under mildly basic conditions. Unfortunately, the anticipated thiol-bearing products could not be isolated.

We subsequently developed another method starting from FP-Tos using NaSH directly as the nucleophile in a $DMF/H_2O$ system. These reaction conditions yielded thiol-derivatized product FP-T (**1**) within short reaction times of only 10−20 min in good yields (Scheme 1). As a result of the basic reaction conditions using NaSH, the dimer of FP-T was initially formed, which could subsequently be reduced efficiently using tris(2-carboxyethyl)phosphine hydrochloride (TCEP), giving the product in good overall yields of 76% after semipreparative HPLC purification.

**Scheme 1. Synthesis of FP-T (1) Starting from Tosyl-fallypride**[a]

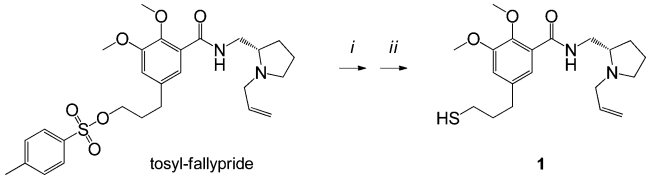


[a]Reagents and conditions: (i) NaSH, $DMF/H_2O$ 3:1, rt; (ii) TCEP, $DMF/H_2O$, rt.

For the first step of this reaction, an exact $DMF/H_2O$ ratio of 3:1 and a small solvent volume just sufficient to dissolve the FP-Tos were found to be critical to obtain the product in high yield and purity. In general, these conditions represent a valuable new complement to former approaches using NaSH for the conversion of tosylates into thiols.[40,41]

**Synthesis of Maleimide-Comprising Peptidic Carriers 2a−22a and Their Reaction with FP-T (1), Yielding Peptide−Fallypride Fusion Molecules 2−22.** Carrier peptide maleimides **2a−22a** were synthesized by standard Fmoc-based solid-phase peptide synthesis (SPPS) using an excess of 3.9 equiv of *O*-(benzotriazol-1-yl)-*N*,*N*,*N*′,*N*′-tetramethyluronium hexafluorophosphate (HBTU) and 4.0 equiv of amino acids and *N*,*N*-diisopropylethylamine (DIPEA) in each conjugation step. The products were obtained in yields of 11−90% after HPLC purification and lyophilization, depending on the complexity of the synthesized peptide.

1,4,7,10-Tetraazacyclododecane-*N*,*N*′,*N*″,*N*‴-tetraacetic acid (DOTA) is a powerful chelator for radiometals such as $^{68}$Ga used for in vivo PET imaging. Thus, some DOTA-derivatized peptides were also synthesized as carriers. $DOTA_{10}$−AngioPep−$PEG_x$−maleimides **9a** and **17a−20a** and DOTA−TfR-$P_s$ maleimide **22a**, all comprising a lysine ε-amino-conjugated DOTA moiety, were synthesized via two different pathways. First, the standard reaction pathway was followed using Fmoc−Lys(Mtt)−OH as an amino acid derivative during the SPPS of peptides **9a** and **22a** followed by Mtt-deprotection under mildly acidic conditions and subsequent conjugation of tris-*t*-Bu-DOTA. However, this strategy gave products **9a** and **22a** in comparatively low yields of 19 and 11%, respectively. Thus, another approach was subsequently used, utilizing the amino acid building block Fmoc−Lys(tris-*t*-Bu-DOTA)−OH (**23**). This chelator-modified amino acid building block was synthesized from $N_\alpha$-Fmoc-protected lysine and tris-*t*-Bu-DOTA using HBTU as an activating agent. Applying this building block in standard SPPS, the respective peptides, **9a**, **17a−20a**, and **22a**, could be obtained in significantly improved but still moderate yields of 20−32% after purification.

Obtained peptide maleimides **2a−22a** were subsequently reacted with FP-T (**1**) in aqueous media at ambient temperature and neutral pH for 10 min (Scheme 2). Products **2−22** were purified by semipreparative HPLC and obtained in yields between 36 and 79%.

**Influence of Different Structural Elements in the Shuttle−Cargo Fusion Molecules on the $hD_2$ Receptor**

**Scheme 2. General Reaction Pathway for the Conjugation Reactions of Peptide Maleimides 2a−22a to FP-T (1), Yielding Peptide−FP-T conjugates 2−22**[a]

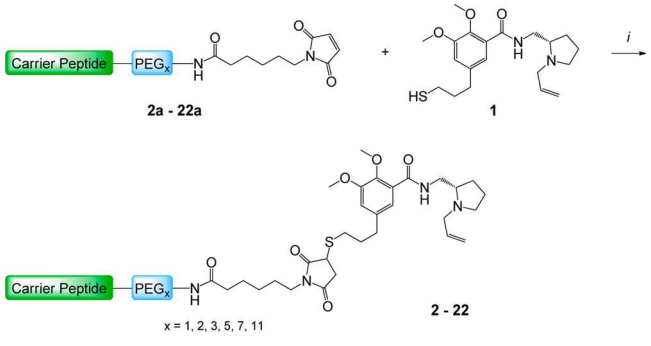


[a]Reagents and conditions: PB/MeCN, pH 6.7−7.2, rt.


dx.doi.org/10.1021/jm5004123 | J. Med. Chem. 2014, 57, 4368−4381

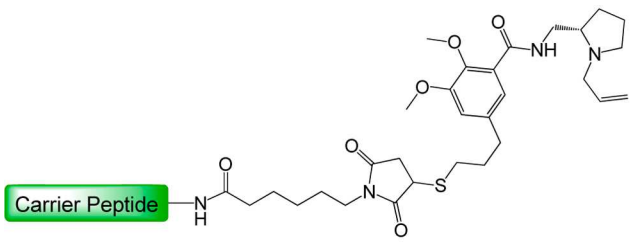


**Carrier Peptides:**

| | |
|---|---|
| TAT (GRKKRRQRRRPPQ) | 2 |
| $TAT_{49-57}$ (RKKRRQRRR) | 3 |
| transferrin receptor binding peptide short (TfR-$P_s$) (HAIYPRH) | 4 |
| transferrin receptor binding peptide long (TfR-$P_l$) (THRPPMWSPVWP) | 5 |
| transportan (GWTLDSAGYLLGKIDLKALAALAKKIL) | 6 |
| penetratin (RQIKIWFQNRRMKWKK) | 7 |
| nuclear localization sequence of human NF-κB (NTP) (VQRKRQKLMP) | 8 |
| $DOTA_{10}$-AngioPep (DOTA-AP) (TFFYGGSRGK(DOTA)RNNFKTEEY) | 9 |

**Figure 2.** Schematic depiction of the synthesized shuttle–cargo fusion molecules of subset **I** (carrier peptide–FP-T fusion molecules **2**–**9**).

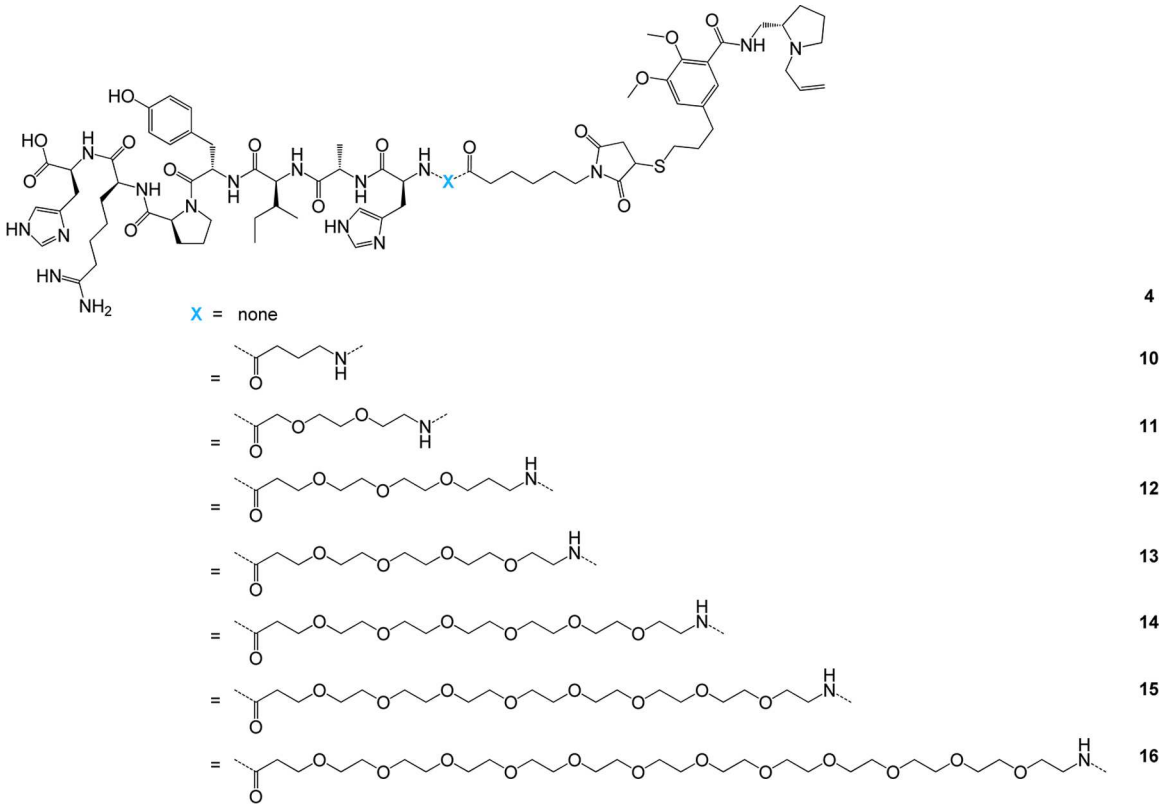


**Figure 3.** Structures of TfR-$P_s$–$PEG_x$–FP-T fusion molecules **4** and **10**–**16** (fusion molecule subset **II**).

**Binding Affinities of the Fallypride Moiety.** In order to determine the influence of peptide architecture as well as potential linkers or other structure elements such as SiFA (silicon fluoride acceptor) and DOTA on the binding affinity of the conjugated fallypride moiety to the $hD_2$ receptor, we synthesized four different subsets of fusion molecules (**I**–**IV**) by systematically varying different structure elements. Subsequently, we determined the binding affinities of these hybrid compounds to the $hD_2$ receptor in vitro.

*Hybrid Molecule Subset I.* This first subset of fusion molecules (**I**) was intended to reveal if the complexity of the carrier peptide exerts a significant influence on the binding parameters of the conjugated fallypride moiety. Thus, different peptidic carriers with the potential to cross the BBB by receptor-mediated processes (TfR-$P_s$, TfR-$P_l$, and AngioPep-2) or transcytosis (TAT, $TAT_{49-57}$, transportan, penetratin, and nuclear localization sequence of NF-κB) of different lengths, amino acid sequence, and complexity were synthesized, derivatized with maleimides, and finally conjugated to FP-T (**1**). The resulting fusion molecules, **2**–**9**, are depicted in Figure 2.

*Hybrid Molecule Subset II.* The second subset was based on the relatively short transferrin receptor binding peptide HAIYPRH (TfR-$P_s$) that has been shown to be able to efficiently enter cells by specific transferrin receptor-mediated transport.[10,42,43] This peptide scaffold was derivatized on a solid support with linkers of different lengths (γ-amino butyric acid, $PEG_1$, $PEG_2$, $PEG_3$, $PEG_5$, $PEG_7$, and $PEG_{11}$) in order to determine if the probable steric hindrance exerted by the peptide on the binding of the fallypride moiety to the $hD_2$ receptor could be attenuated by using an appropriate linker structure. The linker-comprising peptides were reacted on the solid support with maleimido-hexanoic acid, and after cleavage from the resin and purification they were conjugated to FP-T (**1**). The synthesized TfR-$P_s$–$PEG_x$–FP-T fusion molecules, **4** and **10**–**16**, comprising linkers of different length are depicted in Figure 3.

*Hybrid Molecule Subset III.* The third subset of fusion molecules (**III**) was based on the AngioPep-2 peptide that enters the brain by specific receptor-mediated transcytosis utilizing the low-density lipoprotein related receptor LRP1.[17,44,45] Because it has been shown that a derivatization in position $Lys_{10}$ of the peptide is well-tolerated in terms of


dx.doi.org/10.1021/jm5004123 | J. Med. Chem. 2014, 57, 4368–4381

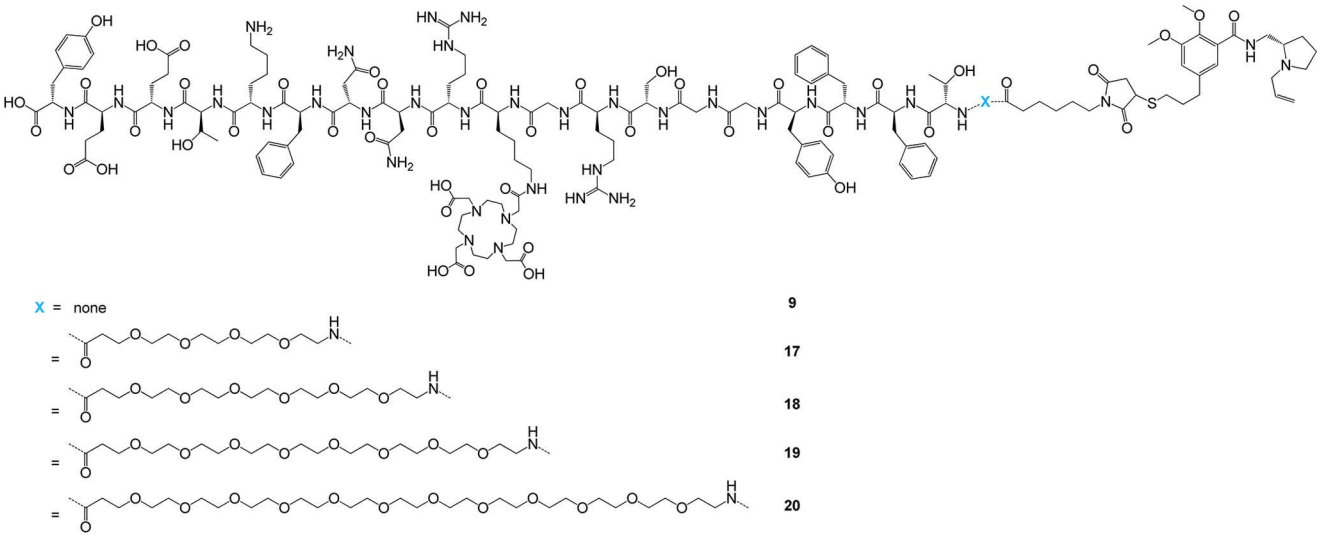


**Figure 4.** Structures of AngioPep−PEG$_x$−FP-T fusion molecules **9** and **17**−**20** (fusion molecule subset **III**).

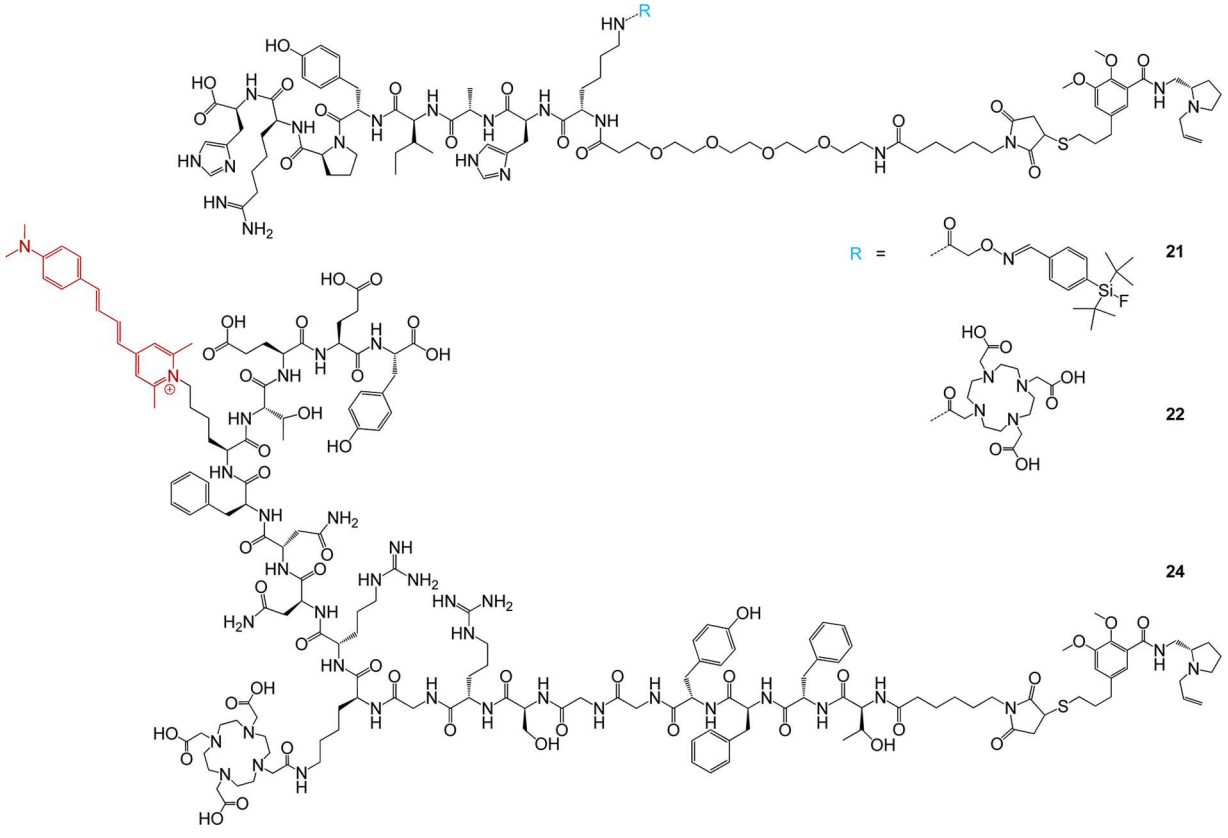


**Figure 5.** Structures of TfR-P$_s$−SiFA−PEG$_3$−FP-T (**21**), TfR-P$_s$−DOTA−PEG$_3$−FP-T (**22**) and DOTA$_{10}$−Py5$_{15}$−AngioPep−FP-T (**24**) (fusion molecule subset **IV**).

AngioPep's transport capacity,[16,18] the chelator DOTA was introduced in this position in all synthesized derivatives. For this purpose, the amino acid building block Fmoc−Lys(tris-*t*-Bu-DOTA)−OH (**23**) was synthesized and implemented into routine Fmoc-SPPS, giving improved yields compared to standard peptide scaffold synthesis, subsequent side-chain deprotection, and chelator functionalization. AngioPep-2 was further reacted on a solid support with PEG linkers of different lengths (PEG$_3$, PEG$_5$, PEG$_7$, and PEG$_{11}$) and maleimido-hexanoic acid. After cleavage from the resin and purification, the peptide derivatives were conjugated to FP-T (**1**). Synthesized AngioPep−PEG$_x$−FP-T fusion molecules **9** and **17**−**20** are shown in Figure 4.

*Hybrid Molecule Subset IV.* Finally, the fourth group of fusion molecules comprised either a SiFA[46−48] or DOTA moiety (for radiolabeling with $^{18}$F or $^{68}$Ga) as well as the near-infrared-emitting fluorescent dye, Py5.[49] These fusion molecules could, in principle, be applicable in in vivo PET imaging or combined PET/optical imaging of hD$_2$ receptors. From these conjugates, it should be possible to determine if the


dx.doi.org/10.1021/jm5004123 | *J. Med. Chem.* 2014, 57, 4368−4381

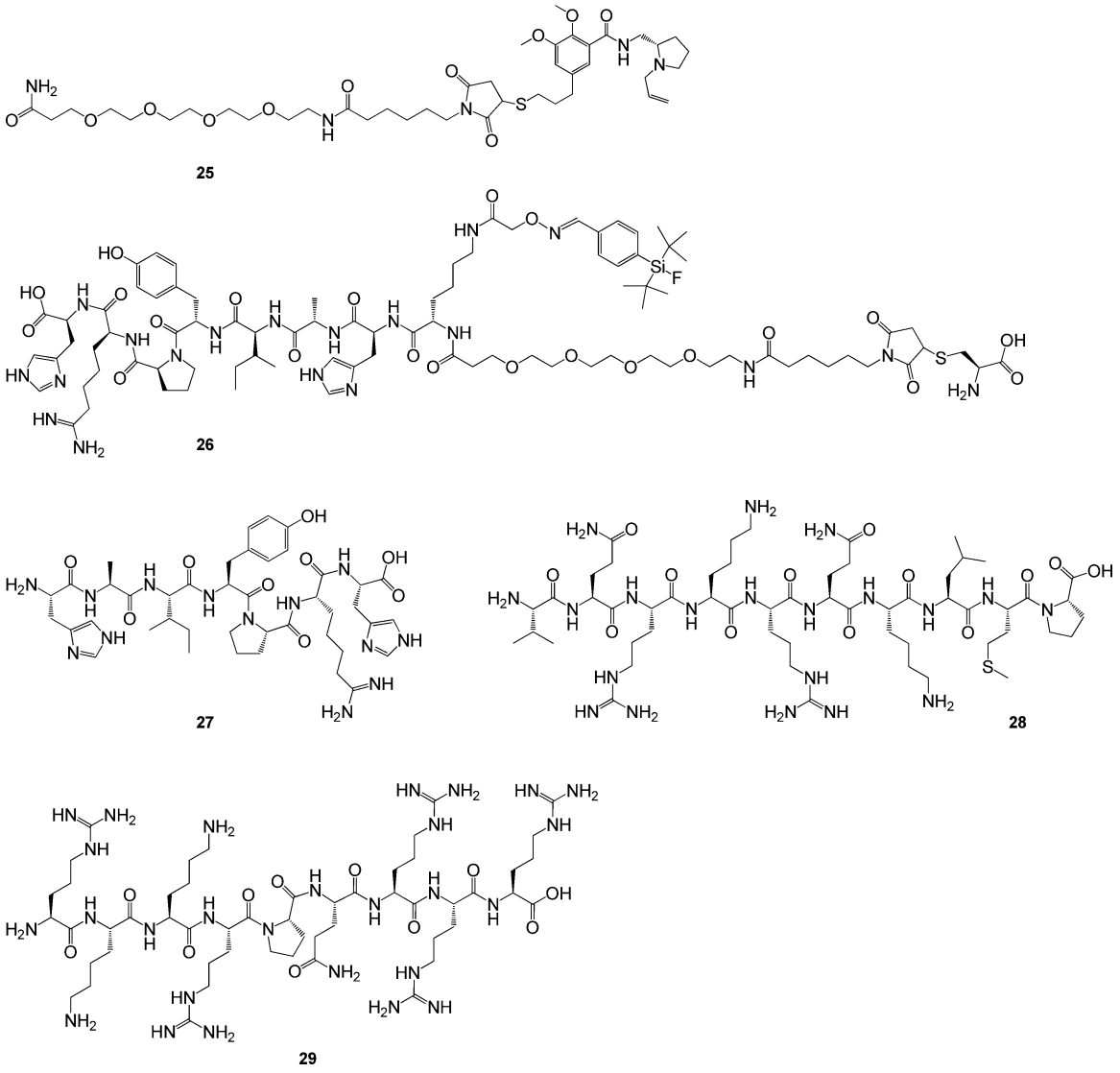


**Figure 6.** Structures $PEG_3$–FP-T (**25**), TfR-$P_s$–SiFA–$PEG_3$–cysteine (**26**), and underivatized TfR-$P_s$ (**27**), TfR-$P_l$ (**28**), and $TAT_{49–57}$ (**29**).

binding affinity of the fallypride moiety to the $hD_2$ receptor tolerates complex structure elements essential for radiolabeling and in vivo imaging such as SiFA, DOTA, and fluorescent dyes introduced within the carrier peptide part of the molecule. Therefore, additional different conjugates based on TfR-$P_s$ and AngioPep-2 were synthesized and derivatized with a SiFA/DOTA and/or Py5 moiety. SiFA-comprising fusion molecule TfR-$P_s$–SiFA–$PEG_3$–FP-T (**21**) was synthesized using Fmoc–Lys(Mtt)–OH during the SPPS. The Mtt protecting group was cleaved under mildly acidic conditions before reacting with *bis*-Boc-aminooxy-acetic acid using the standard coupling protocol on solid support. The peptide was then modified with the $PEG_3$-linker and maleimido-hexanoic acid, cleaved from the solid support, and reacted with SiFA-A, an aldehyde-bearing SiFA building block,[48,50] and FP-T (**1**) after purification. **22** was synthesized as described earlier. The DOTA and Py5 near-infrared fluorescent dye comprising fusion molecule **24** was obtained by reaction of $DOTA_{10}$–AngioPep–FP-T (**9**) with Py5. Obtained fusion molecules **21**, **22**, and **24** are depicted in Figure 5.

*Synthesis of Control Substances.* In order to exclude an unlikely but theoretically possible nonspecific interaction of the peptide/linker/2,5-dioxo-3-pyrrolidinyl-thioether/lipophilic SiFA structure of the fusion molecules with the $hD_2$ receptor, we prepared various negative control compounds that were also evaluated in vitro with regard to their binding affinities to the $hD_2$ receptor.

TfR-$P_s$–SiFA–$PEG_3$–cysteine (**26**) was obtained by reaction of **21a** with cysteine in order to obtain a very structurally similar analogue to **21** that is, however, not able to specifically bind to the $hD_2$ receptor because it lacks the fallypride moiety, but it retains the peptide, PEG linker, SiFA moiety, and 2,5-dioxo-3-pyrrolidinyl-thioether. Furthermore, underivatized TfR-$P_s$ (**27**), TfR-$P_l$ (**28**), and $TAT_{49–57}$ (**29**) as well as a $PEG_3$–FP-T (**25**, as a specific binding control) were synthesized and tested for their in vitro binding affinities to the $hD_2$ receptor together with fusion molecules **2**–**22**, **24**, and **26**. The structures of control substances **25**–**29** are presented in Figure 6.

**Radiolabeling of Fusion Molecules 9, 17–22, and 24 with $^{18}F$ and $^{68}Ga$.** In principle, the synthesized fusion molecules could be interesting candidates for in vivo imaging of the $hD_{2/3}$ receptor system with PET. Consequently, some of the conjugates were designed bearing a SiFA[46–48] or DOTA


dx.doi.org/10.1021/jm5004123 | J. Med. Chem. 2014, 57, 4368–4381

moiety in order to be amenable to direct radiolabeling with $^{18}F$ and $^{68}Ga$, respectively. In the following radiolabeling study, we investigated whether SiFA- and DOTA-comprising fusion molecules **9**, **17**–**22**, and **24** are de facto amenable to radiolabeling with $^{18}F$ and $^{68}Ga$.

The radiolabeling of the fusion molecule $DOTA_{10}$–$Py5_{15}$–AngioPep–FP-T (**24**) with $^{68}Ga^{3+}$ gave only poor radiolabeling results under standard reaction conditions, as several unidentified radioactive byproducts were formed that could not be easily separated by HPLC. Because labeling precursor **24** is structurally identical to **9** (apart from the near-infrared fluorescent dye Py5 being introduced into the $N_\varepsilon$-$Lys_{15}$ amino side chain functionality of the peptide), which can be labeled efficiently using standard conditions as described below, the formation of byproducts seems to be a result of the sensitivity of the large delocalized system of $\pi$ electrons within the fluorescent dye. Thus, a derivative being amenable to $^{68}Ga$ labeling for PET imaging as well as to optical imaging simultaneously would require the use of a different, less sensitive near-infrared fluorescent dye.

Also, when radiolabeling the fusion molecule TfR-$P_s$–SiFA–$PEG_3$–FP-T (**21**) with $^{18}F^-$, several unidentified radioactive byproducts were formed, resulting in only poor radiolabeling results under standard reaction conditions. Similar byproducts as those observed in the $^{18}F$ labeling of **21** were also observed for a structurally similar fusion molecule of TfR-$P_s$ and a SiFA moiety conjugated via a 2,5-dioxo-3-pyrrolidinyl-thioether structure (SiFA–*S*-maleimido–THRPPMWSPVWP).[51] Because neither the presence of peptides comprising various side chain functionalities nor PEG linkers nor fallypride interfere with the used $^{18}F$-SiFA-labeling conditions,[52,53] it can be inferred from these data that the 2,5-dioxo-3-pyrrolidinyl-thioether structure element is sensitive to the slightly basic labeling conditions used, resulting in the formation of structurally similar, perhaps ring opening, byproducts. In order to circumvent the formation of these byproducts, milder $^{18}F$-labeling conditions were applied, resulting in the formation of the desired product, [$^{18}F$]**21**, only. These reaction conditions apply the so-called Munich method for cartridge-based [$^{18}F$]fluoride drying[54] and a subsequent in part neutralization of the reaction mixture with oxalic acid, which has been shown to give excellent radiolabeling results.[48] Under these conditions, the only byproduct is unreacted [$^{18}F$]fluoride, which can be easily removed by cartridge purification, giving final product [$^{18}F$]**21** in radiochemical yields of up to 60%, radiochemical purities of ≥98%, and specific activities of up to 80 GBq/$\mu$mol (2160 mCi/$\mu$mol) in an overall synthesis time of only 25 min.

The $^{68}Ga$ labeling of fusion molecules **9**, **17**–**20**, and **22** proceeded efficiently, giving the radiolabeled products in high radiochemical yields and purities of 96–98% as well as in high specific activities of 19.2–28.1 GBq/$\mu$mol (519–759 mCi/$\mu$mol) using standard labeling conditions.

**Determination of $hD_2$ Receptor Binding Affinities of 2–22 and 24–29.** Fusion shuttle–carrier fusion molecules **2**–**22** and **24** as well as control substances **25**–**29** were tested in vitro for their $hD_2$ receptor binding affinity in an established competition binding assay by displacement of [$^3$H]spiperone on human $D_2$ receptor-transfected HEK cells.[51,55] This is an established procedure, with the obtained affinities giving a valuable indication of the biological potency of the newly developed receptor ligands. All binding experiments were performed at least thrice separately, with each experiment being carried out in triplicate. The binding affinity of fallypride derivative **1** could not be determined because it showed considerable dimerization under the conditions of the in vitro binding experiment that would have falsified the results. Fallypride (FP), desmethoxy-fallypride (DMFP), raclopride (RP), haloperidol (HP), chlorpromazine (CP), and (+)-butaclamol (BC) were coevaluated as reference compounds. Table 1 summarizes the results of these evaluations.

**Table 1. $K_i$ Values of Compounds 2–22 and 24–29 and Internal Standards[b]**

| Compd. | $K_i$ ± SEM [nM] | Compd. | $K_i$ ± SEM [nM] |
|---|---|---|---|
| **2** | 21.47 ± 3.14 | **19** | 42.80 ± 2.75 |
| **3** | 9.69 ± 2.26 | **20** | 44.67 ± 11.4 |
| **4** | 10.32 ± 1.39 | **21** | 5.98 ± 1.11 |
| **5** | 27.32 ± 6.77 | **22** | 52.03 ± 6.63 |
| **6** | 12.27 ± 3.67 | **24** | 64.16 ± 18.54 |
| **7** | 8.14 ± 0.55 | **25** | 7.31 ± 0.95 |
| **8** | 12.96 ± 2.30 | **26** | › 1,000 [a] |
| **9** | 8.01 ± 2.61 | **27** | › 1,000 [a] |
| **10** | 28.43 ± 5.35 | **28** | › 1,000 [a] |
| **11** | 30.33 ± 5.35 | **29** | › 1,000 [a] |
| **12** | 23.78 ± 5.56 | | |
| **13** | 1.47 ± 0.38 | **FP** | 0.097 ± 0.015 |
| **14** | 27.39 ± 9.50 | **BC** | 0.37 ± 0.13 |
| **15** | 53.92 ± 8.69 | **DMFP** | 0.63 ± 0.09 |
| **16** | 25.27 ± 3.41 | **HP** | 0.85 ± 0.12 |
| **17** | 26.13 ± 4.47 | **RP** | 1.21 ± 0.43 |
| **18** | 35.77 ± 3.73 | **CP** | 6.10 ± 1.39 |

[a]Concentrations of up to 1 $\mu$M were studied and showed no displacement of [$^3$H]spiperone. Abbreviations: FP, Fallypride; DMFP, desmethoxy-fallypride; RP, raclopride; HP, haloperidol; CP, chlorpromazine; and BC, (+)-butaclamol. [b]Yellow, fusion molecule subset **I**; orange, fusion molecule subset **II**; green, fusion molecule subset **III**; blue, fusion molecule subset **IV**; violet, positive and negative controls; and grey, internal standards.

As can be seen from the in vitro data, the binding affinity of the fallypride moiety to the $hD_2$ receptor is still in the nanomolar range (between 1.5 and 64.2 nM) for all studied compounds and thus it is in a comparable range to that of raclopride (affinity: 1.2 nM) and chlorpromazine (affinity: 6.1 nM), although the affinity is markedly reduced upon conjugation to complex structural systems such as peptides. This is remarkable insofar as a more pronounced reduction of binding affinities was expected, especially in the case of large peptidic carriers that were hypothesized to considerably hamper the fallypride moiety from binding to the $hD_2$ receptor by folding effects, steric hindrance, or entropy effects.

As expected, fusion molecule **26** (comprising all structure elements of high-affinity binder **21** except for the fallypride moiety: TfR-binding peptide, PEG linker, lipophilic SiFA moiety, and 2,5-dioxo-3-pyrrolidinyl-thioether) and unmodified peptides **27**–**29** showed no affinity to the $hD_2$ receptor in the


dx.doi.org/10.1021/jm5004123 | J. Med. Chem. 2014, 57, 4368–4381

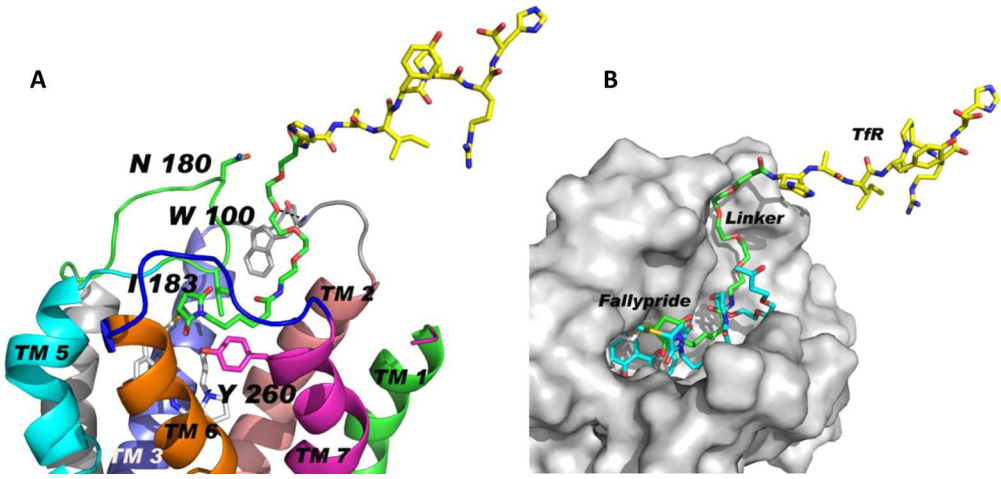


**Figure 7.** (A) Predicted binding mode of **13** to the model $hD_2$ receptor obtained from 6 ns MD simulations. The fallypride part of compound **13** is depicted in original atom color, the linker part, in green, and the peptidic part (TfR-binding peptide), in yellow. (B) Overlay of the energy-minimized MD average structures of **25** (in cyan carbon atoms) and **13** (fallypride is depicted in original atom color, linker structure, in green, and peptide, in yellow) bound to the $hD_2$ receptor. The $hD_2$ receptor is displayed as a molecular surface in gray for improved clarity.

studied concentration range of up to 1 $\mu$M. This conclusively demonstrates that the observed high $hD_2$ receptor binding affinities of the fusion molecules are a result of the fallypride structure element and thus specific binding.

The complexity, length, and individual structure of the used peptidic carriers (studied within subset **I**; compounds **2**−**9**) seems to have no significant influence on the binding affinities of the conjugated fallypride moiety. Fusion molecules comprising very short peptides such as **4** exhibit comparable affinities (10.3 nM) as that of very complex ones such as **7** or **6** (8.1 and 12.3 nM, respectively). This is further corroborated by the results obtained for compound **9**, for which a relatively high affinity of 8.0 nM was observed (which is the highest observed affinity within this subgroup) despite the rather long peptide sequence, the variety in hydrophilic as well as lipophilic amino acid side chain functionalities, and the additional chelator structure within the peptide sequence.

Regarding the linker length, whose influence was studied within the subsets **II** (compounds **4** and **10**−**16**) and **III** (compounds **9** and **17**−**20**) using the transferrin receptor-affine peptide TfR-$P_s$ and AngioPep as scaffold peptides, significant effects of linker lengths on binding affinities were observed. Within TfR-$P_s$−$PEG_x$−FP-T subgroup **II**, the best results were found for **13** (binding affinity of 1.5 nM), whereas shorter or longer linkers resulted in lower affinities between 10.3 and 53.9 nM, which might be attributable to suboptimal receptor penetration depths in the case of short linkers and entropy costs in the case of long linkers.

However, different results were obtained within AngioPep−$PEG_x$−FP-T series **III**, where the highest binding affinity of 8.0 nM was found for derivative **9** that does not have any linker structure at all. The introduction of a linker in this subset resulted in affinities moderately decreasing from 26.1 to 44.7 nM with increasing linker lengths.

Thus, the linker length resulting in optimal binding parameters in such fusion molecules has to be determined for each peptide system independently.

A considerable influence on binding affinities was also observed for the conjugation of SiFA, DOTA, and Py5 within the peptide carrier sequence that was studied in subgroup **IV**, including fusion molecules **21**, **22**, and **24**. The conjugation of a $^{18}$F-binder or NIR dye resulted in a markedly decreased binding affinity in the case of the introduction of a small lipophilic SiFA or Py5 moiety (6.0 nM for **21** instead of 1.5 nM for its lead compound, **13**, and 64.2 nM for **24** instead of 8.0 nM in the case of its lead compound, **9**) and even a significant decrease in affinity in the case of the introduction of a hydrophilic and sterically demanding DOTA moiety (52.0 nM for **22** instead of 1.5 nM in case of its lead compound, **13**). The strong reduction of affinity observed in the case of DOTA introduction into the peptide sequence of TfR-$P_s$ (**22**) interestingly does not seem to be a result of the position of conjugation (the introduction of the SiFA moiety in the same position (**21**) did not result in such a marked decrease of binding affinity) but might be a consequence of the higher hydrophilicity/charge of the DOTA moiety compared to that of the SiFA scaffold.

**Molecular Modeling of the $hD_2$ Receptor and Docking Studies.** As a more pronounced reduction in the binding affinities of fallypride to the human $D_2$ receptor was expected upon conjugation to large and complex peptidic carriers, we also performed homology modeling of the receptor and docking studies of selected compounds (fallypride, **25**, and **13**; detailed information is available in the Supporting Information). By this, we intended to determine the influence of the different structure elements of the fusion molecules on $hD_2$ receptor binding and to elucidate the reason for the experimentally observed preserved binding of the hybrid molecules.

When docking hybrid molecule **13** to the modeled $hD_2$ receptor, the peptide, in contrast to the PEG linker, does not seem to contribute to the stabilization of fusion molecule binding to the $hD_2$ receptor, as it is mostly exposed to solvent. The predicted binding of **13** to the $hD_2$ receptor is depicted in Figure 7A,B and shows an overlay of the predicted binding modes of **25** and **13** for direct comparison.

Hence, this in silico modeling shows that the fallypride moiety of the fusion molecules is still able to bind in its binding pocket of the $hD_2$ receptor and that the linker and peptide do not seem to negatively influence the ligand binding by not directly interacting with the binding pocket of the receptor. On the contrary, it indicates that the PEG linker might contribute to the observed preserved binding properties of the fallypride


dx.doi.org/10.1021/jm5004123 | J. Med. Chem. 2014, 57, 4368−4381

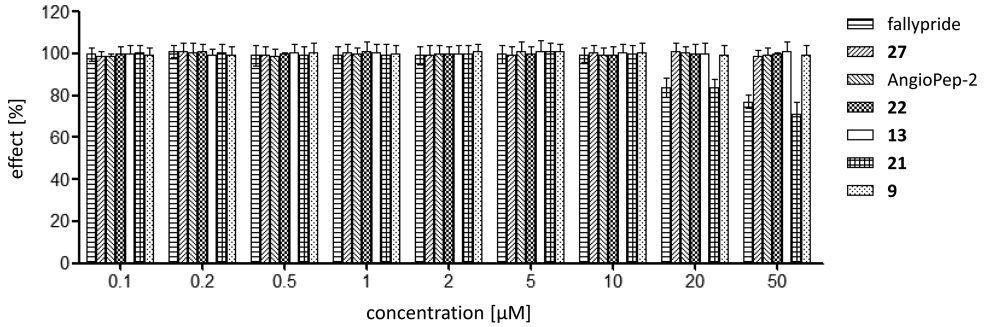


**Figure 8.** Results obtained from the Calcein assay to identify the interaction of the studied substances with P-gp. Intracellular fluorescence in the absence of test compounds was set as 100%. None of the substances showed any modulation of P-gp in the concentration range of 0.1−10 $\mu$M. At higher concentrations, fallypride as well as **21** showed an interaction with the applied esterase, disturbing the assay at concentrations >10 $\mu$M and resulting in the lower fluorescence values observed, which are not consequence of P-gp modulation by these compounds. Cyclosporine A was used as a positive control and showed an $IC_{50}$ value of 0.94 $\mu$M under the same conditions.

moiety by creating a spatial separation between the binding ligand and the peptidic carrier.

These results obtained in silico thus support the three main experimentally observed effects: (i) the retained binding affinity of the hybrid molecules to the $hD_2$ receptor, (ii) the increased affinity of PEG linker-modified hybrid molecules when optimizing linker lengths, and (iii) the missing influence of the peptide size and complexity on the fallypride binding (Table 1).

**Estimation of the Blood−Brain Barrier Permeability of Hybrid Compounds 9, 13, 21, and 22, Native TfR-Binding Peptide, AngioPep-2, and Fallypride.** After having shown that the conjugation of a small neuroreceptor-affine drug to a transport peptide can result in a hybrid compound that is still able to bind its target receptor, we intended to estimate the potential of the developed fusion molecules to enter the brain parenchyma. The BBB is the last hurdle for the hybrid compounds in the studied molecular Trojan horse approach using covalent conjugates of receptor-affine small molecules and peptides as carriers. On the molecular level, the P-glycoprotein transporter protein (P-gp) is known to play the major role in the development of drug resistance that is associated with limited CNS permeation of drug candidates.[56] Because of its broad substrate spectrum and high expression level at various blood−tissue barriers, P-gp considerably affects the pharmacokinetics and bioavailability of various agents.

The Calcein cell assay is a highly sensitive, specific, and reliable screening method that allows for the rapid evaluation and classification of drug candidates according to their P-gp interaction.[56] A key detection component in this assay is the Calcein−acetoxymethylester (Calcein-AM) complex that is easily internalized in cells and acts as a substrate of both P-gp and intracellular esterases. In the presence of a P-gp inhibitor or substrate, the transporter binding sites are occupied, and as a result, the Calcein-AM complex cannot interact with P-gp. In this case, Calcein-AM is not transported out of the cells and is hydrolyzed to the fluorescent product, Calcein, by the activity of cellular esterases. Depending on the P-gp affinity of certain test compounds, the amount of Calcein formation reaches different levels at specific compound concentrations. The level of the fluorophore formation serves as an indicator to determine the P-gp interaction profile of the given test compounds.[56,57] In this study, we used the human brain endothelial capillary cell line hCMEC/D3 that exhibits stable expression of P-gp.[58] In order to verify the assay, we used known P-gp inhibitor cyclosporine A as an internal positive control.

In this assay, we studied the most promising hybrid molecules, **9**, **13**, **21**, and **22**, as well as their native peptide lead structures **27**, AngioPep-2, and the receptor ligand fallypride as references and Cyclosporine A as positive control.

*Determination of the Toxicity of the Substances.* In order to exclude the possibility that the tested compounds are toxic to the cells and thus falsifying the Calcein assay, the cytotoxicity of the compounds was evaluated in an AlamarBlue assay that identifies cytotoxic substances by their ability to decrease the metabolic activity and thus the redox potential of viable cells. The assay revealed no cytotoxic effects for any of the tested compounds on hCMEC/D3 cells (Figure S1, Supporting Information).

*Determination of the Interaction of Hybrid Molecules and P-glycoprotein.* The interaction of the substances with P-gp was studied by subjecting them to the Calcein assay, which is a highly sensitive, specific, and reliable screening method that allows for the rapid evaluation and classification of drug candidates according to their P-gp interaction.[56,57] Intracellular accumulation of free Calcein corresponds to the degree of P-gp interaction of a given test compound. For this assay, the hCMEC/D3 cell line was used, which is known to stably express P-gp.[58] The P-gp inhibitor, Cyclosporine A, served as an internal positive control.

None of the studied substances, neither hybrid molecules nor native peptides nor fallypride, were substrates of P-gp (Figure 8), implying that they are not transported from the abluminal to the luminal side of the endothelium by P-gp. Although this assay is not able to reproduce the complex situation in a living subject, these results indicate that the transport of the developed fusion molecules over the BBB is not prevented by the main excretory transporter of the BBB, P-gp.

## ■ CONCLUSIONS

From the obtained results, it can be inferred that even a small neuroreceptor ligand such a fallypride binding to the $hD_{2/3}$ receptor can be conjugated to a relatively large peptidic carrier molecule while largely retaining its nanomolar binding affinity to the target receptor (specific binding affinities of up to 1.5 nM were found in this study).

These promising experimental in vitro results were further substantiated by in silico molecular modeling studies that indicated that the fallypride moiety of the fusion molecules is

still able to bind to its binding pocket of the $hD_2$ receptor. Despite the significant structural changes exerted by conjugation, neither linker nor peptide seem to negatively influence the ligand binding to its receptor. The linker can even slightly stabilize the ligand−receptor interaction according to the in silico modeling.

Furthermore, the most promising hybrid substances were tested to determine if they possibly interact with P-gp, showing that these substances are not substrates of this transporter. This indicates that the transcytosis of the developed fusion molecules over the BBB is not prevented by its main excretory transporter, P-gp.

These findings should encourage enlarging the research focus of molecular Trojan horse drug delivery across the BBB from the generally used proteins toward transport peptides as carriers.

## EXPERIMENTAL SECTION

**General.** All commercially available chemicals were of analytical grade and were used without further purification. Resins for peptide synthesis, coupling reagents, and Fmoc-protected amino acids were purchased from NovaBiochem. Calcein and Cyclosporine A were purchased at the highest purity grade from Sigma-Aldrich. EBM-2 basal medium and Single-Quot Kit were obtained from Lonza, fetal bovine serum, from Biochrom, and rat-tail collagen type I, from Hoffmann-LaRoche. SiFA-A, Py5, and tosyl-fallypride were synthesized as described elsewhere.[39,50,59] For analytical and semipreparative HPLC chromatography, an Agilent 1200 system or a Dionex 3000 HPLC system equipped with a Gabi-Star (Raytest) radioactivity detector was used. The columns used for chromatography were Chromolith Performance (RP-18e, 100−4.6 mm, Merck, Germany) and Chromolith (RP-18e, 100−10 mm, Merck, Germany) columns, operated with flows of 4 and 8 mL/min, respectively. The preparative HPLC system used was a Knauer Preparative Pump 1800 together with a Knauer Smartline UV detector 2600 and a Chromolith Prep (RP-18e, 100−25 mm, Merck, Germany) column, operated with a flow of 100 mL/min. ESI, MALDI, and NMR spectra were obtained with a Finnigan MAT95Q, a Bruker Daltonics Microflex, and a Jeol AS500 spectrometer, respectively.

The purity of synthesized compounds **1**, **2a**−**22a**, and **2**−**29** was ≥96% in each case, as determined by analytical HPLC.

The determination of the FP-T−peptide conjugate binding affinities to the human $D_2$ receptor was performed by competition binding experiments according to a previously described procedure.[51]

A detailed description of homology modeling of the $hD_2$ receptor, model prediction, docking studies, and molecular dynamics simulations as well as a detailed description of the cytotoxicity and Calcein assays can be found in the Supporting Information.

**Synthesis of 3-(3-((1-Allylpyrrolidin-2-yl)methylcarbamoyl)-4,5-dimethoxy-phenyl)-propyl-thiol (FP-T, 1).** A solution of sodium hydrosulfide (217 mg, 3.87 mmol) in DMF/$H_2O$ (3:1, 1 mL) was added to a solution of tosyl-fallypride (200 mg, 387 μmol) in DMF (650 μL). The initially dark green color of the solution bleached within 10 to 15 min, indicating the end of the reaction. After addition of $H_2O$ (1 mL), Tris(2-carboxyethyl)phosphine hydrochloride (TCEP) (∼150 mg) was added as a solid until gas formation stopped. The crude product was purified by semipreparative HPLC using a gradient of 0−40% MeCN + 0.1% FA over 6 min. The product was obtained as colorless oil after lyophilization (111 mg, 293 μmol, 76%). $^1$H NMR (acetone-$d_6$): δ 8.56 (bs, 1H), 7.35−7.32 (m, 1H), 7.10−7.07 (m, 1H), 6.13−6.03 (m, 1H), 5.53 (d, 1H, $J^2$ = 16.5), 5.41 (d, 1H, $J^2$ = 10.3), 4.06−4.02 (m, 1H), 3.92 (s, 3H), 3.90 (s, 3H), 3.89−3.70 (m, 4H), 3.23−3.16 (m, 1H, $J^3$ = 7.7), 2.72 (t, 2H, $J^3$ = 7.7), 2.68−2.46 (m, 4H), 2.36−2.31 (m, 1H), 2.13−2.07 (m, 2H), 2.01−1.82 (m, 2H), 1.77 (t, 1H, $J^3$ = 7.9). $^{13}$C NMR (acetone-$d_6$): δ 166.89, 153.68, 146.88, 138.29, 129.24, 127.48, 124.69, 122.20, 116.73, 66.82, 61.52, 58.07, 56.41, 54.41, 41.53, 36.46, 34.71, 29.11, 24.26, 23.53. ESI-MS ($m/z$) for $[M + H]^+$ (calcd): 379.20 (379.20).

**General Synthesis of Carrier Peptide Maleimides 2a−20a.** Peptides were synthesized on solid support by standard Fmoc solid-phase peptide synthesis as described by Wellings et al.[60] using standard commercially available resins, amino acids, Fmoc−amino−PEG−acids and Fmoc−Lys(tris-*t*-Bu-DOTA)−OH (**23**). The N-terminal modification with maleimido-hexanoic acid was accomplished using the standard coupling protocol for amino acids after cleavage of the N-terminal Fmoc protecting group. The resulting maleimide-modified peptides were cleaved from the solid support using a mixture of TFA (trifluoroacetic acid)/TIS (triisopropylsilane)/$H_2O$ (95:2.5:2.5) for 90 min, suspended in diethyl ether, and purified by semipreparative HPLC. The products were isolated as white solids after lyophilization. Gradients used for HPLC purification and overall synthesis yields are given below.

**2a**: gradient, 0−30% MeCN in 6 min; yield, 90%; MALDI-MS ($m/z$) for $[M + H]^+$ (calcd): 1912.2 (1912.1). **3a**: gradient, 0−30% MeCN in 6 min; yield, 72%; ESI-MS ($m/z$) for $[M + 2H]^{2+}$ (calcd): 738.92 (766.97). **4a**: gradient, 15−40% MeCN in 6 min, yield: 76%; ESI-MS ($m/z$) for $[M + H]^+$ (calcd): 1085.55 (1085.55), ($m/z$) for $[M + 2H]^{2+}$ (calcd): 543.28 (543.27). **5a**: gradient, 20−45% MeCN in 6 min; yield, 44%; MALDI-MS ($m/z$) for $[M + H]^+$ (calcd): 1683.6 (1683.8). **6a**: gradient, 30−80% MeCN in 6 min; yield, 11%; MALDI-MS ($m/z$) for $[M + H]^+$ (calcd): 3040.6 (3035.8). **7a**: gradient, 15−40% MeCN in 6 min; yield, 28%; ESI-MS ($m/z$) for $[M + 3H]^{3+}$ (calcd): 814.13 (832.80), ($m/z$) for $[M + 4H]^{4+}$ (calcd): 610.85 (624.85). **8a**: gradient, 15−40% MeCN in 6 min; yield, 83%; ESI-MS ($m/z$) for $[M + H]^+$ (calcd): 1476.84 (1476.84), ($m/z$) for $[M + 2H]^{2+}$ (calcd): 738.92 (738.92). **9a**: gradient, 0−50% MeCN in 6 min; yield, 31%; ESI-MS ($m/z$) for $[M + H + Na + K_{complexed}]^{2+}$ (calcd): 1471.64 (1471.66), ($m/z$) for $[M + 2H + Na + K_{complexed}]^{3+}$ (calcd): 981.10 (981.11). **10a**: gradient, 0−30% MeCN in 6 min; yield, 69%; ESI-MS ($m/z$) for $[M + H]^+$ (calcd): 1170.60 (1170.60), ($m/z$) for $[M + 2H]^{2+}$ (calcd): 585.80 (585.80). **11a**: gradient, 0−30% MeCN in 6 min; yield, 73%; ESI-MS ($m/z$) for $[M + H]^+$ (calcd): 1230.62 (1230.62), ($m/z$) for $[M + 2H]^{2+}$ (calcd): 616.31 (615.81). **12a**: gradient, 0−30% MeCN in 6 min; yield, 61%; ESI-MS ($m/z$) for $[M + H]^+$ (calcd): 1288.66 (1288.66), ($m/z$) for $[M + 2H]^{2+}$ (calcd): 644.83 (644.83). **13a**: gradient, 0−30% MeCN in 6 min; yield, 65%; ESI-MS ($m/z$) for $[M + H]^+$ (calcd): 1332.69 (1332.69), ($m/z$) for $[M + 2H]^{2+}$ (calcd): 666.85 (666.85). **14a**: gradient, 0−30% MeCN in 6 min; yield, 84%; ESI-MS ($m/z$) for $[M + H]^+$ (calcd): 1420.74 (1420.74), ($m/z$) for $[M + 2H]^{2+}$ (calcd): 710.87 (710.87). **15a**: gradient, 10−40% MeCN in 6 min; yield, 71%; ESI-MS ($m/z$) for $[M + H]^+$ (calcd): 1508.80 (1508.79), ($m/z$) for $[M + 2H]^{2+}$ (calcd): 754.90 (754.90). **16a**: gradient, 10−40% MeCN in 6 min; yield, 73%; ESI-MS ($m/z$) for $[M + H]^+$ (calcd): 1684.90 (1684.90), ($m/z$) for $[M + 2H]^{2+}$ (calcd): 842.95 (842.95). **17a**: gradient, 0−40% MeCN in 6 min; yield, 32%; substance was directly reacted with FP-T after reduction of solvent volume. **18a**: gradient, 0−40% MeCN in 6 min; yield, 31%; substance was directly reacted with FP-T after reduction of solvent volume. **19a**: gradient, 0−40% MeCN in 6 min; yield, 31%; substance was directly reacted with FP-T after reduction of solvent volume. **20a**: gradient, 0−40% MeCN in 6 min; yield, 22%; substance was directly reacted with FP-T after reduction of solvent volume.

**Synthesis of TfR-$P_s$−SiFA−$PEG_3$−Maleimide 21a.** TfR-$P_s$ (50 μmol) was synthesized on solid support as described above. Fmoc−Lys(Mtt)−OH was coupled using the standard coupling protocol after removal of the N-terminal Fmoc protecting group followed by coupling of Fmoc−$PEG_3$−OH and maleimido-hexanoic acid. For selective deprotection of the terminal lysine side chain functionality, the Mtt protecting group was cleaved using TFA (1.75%) and TIS (1%) in DCM, and the resulting charged ammonium group was converted into the amine by treatment with DIPEA in DCM (2%, 6 × 2 mL) before reacting with *bis*-Boc-aminooxy-acetic acid using the standard coupling protocol. The peptide was cleaved from the solid support, deprotected, and purified by semipreparative HPLC using a gradient of 0−40% MeCN + 0.1% FA over 6 min. The product was obtained as a white solid after lyophilization (15.6 mg, 10.2 μmol, 20%). ESI-MS ($m/z$) for $[M + H]^+$ (calcd): 1533.80 (1533.80), ($m/z$) for $[M + 2H]^{2+}$ (calcd): 767.40 (767.40). Subsequently, a solution of


dx.doi.org/10.1021/jm5004123 | J. Med. Chem. 2014, 57, 4368−4381

this aminooxy-functionalized intermediate (9.4 mg, 6.13 μmol) in PB (0.5 M, pH 4, 150 μL) was added to a solution of SiFA-A (3.26 mg, 12.26 μmol) in MeCN (300 μL). After 10 min, the crude product was purified by semipreparative HPLC using a gradient of 20−90% MeCN + 0.1% FA over 6 min. The product was obtained as a white solid after lyophilization (5.3 mg, 2.98 μmol, 49%). ESI-MS ($m/z$) for $[M - H]^-$ (calcd): 1781.92 (1781.94).

**Synthesis of TfR-$P_s$−DOTA−$PEG_3$−Maleimide 22a.** TfR-$P_s$ (50 μmol) was synthesized on solid support as described above. Fmoc−Lys(tris-*t*-Bu-DOTA)−OH (**23**) was introduced using the standard coupling protocol after removal of the N-terminal Fmoc protecting group followed by coupling of Fmoc−$PEG_3$−OH and maleimido-hexanoic acid. The peptide was cleaved from the solid support, deprotected, and purified by semipreparative HPLC using a gradient of 0−40% MeCN + 0.1% FA over 6 min. The product was obtained as a white solid after lyophilization (18.3 mg, 9.91 μmol, 20%). ESI-MS ($m/z$) for $[M + H + Na_{salt} + K_{complexed}]^+$ (calcd): 1909.88 (1909.93), ($m/z$) for $[M + 2H + Na_{salt} + K_{complexed}]^{2+}$ (calcd): 954.94 (954.97).

**General Synthesis of Carrier Peptide−FP-T Conjugates 2−22.** To a solution of peptide maleimides **2a**−**22a** (2.5−10 μmol) in PB (phosphate buffer, 0.1 M, pH 4.0)/MeCN 1:1 (250 μL) was added a solution of FP-T (**1**, 1.25 equiv) in MeCN, and the pH of the solution was adjusted to 6.7−7.2 using PB (0.5 M, pH 7.2, ∼ 50 μL). After 10 min, the reactions were complete, and the crude products were purified by semipreparative HPLC. The products were isolated as white solids after lyophilization. Gradients used for HPLC purification and overall synthesis yields are given below.

**2**: gradient, 0−40% MeCN in 6 min; yield, 71%; MALDI-MS ($m/z$) for $[M + H]^+$ (calcd): 2291 (2289). **3**: gradient, 15−40% MeCN in 6 min; yield, 67%; ESI-MS ($m/z$) for $[M + 4H]^{4+}$ (calcd): 478.54 (478.53). **4**: gradient, 15−50% MeCN in 6 min; yield, 56%; ESI-MS ($m/z$) for $[M + 2H]^{2+}$ (calcd): 732.37 (732.37). **5**: gradient, 20−45% MeCN in 6 min; yield, 62%; ESI-MS ($m/z$) for $[M + 2H]^{2+}$ (calcd): 1031.51 (1031.50), ($m/z$) for $[M + 3H]^{3+}$ (calcd): 688.01 (688.00). **6**: gradient, 30−80% MeCN in 6 min; yield, 36%; MALDI-MS ($m/z$) for $[M + H]^+$ (calcd): 3414.8 (3413.9). **7**: gradient, 15−40% MeCN in 6 min; yield, 69%; ESI-MS ($m/z$) for $[M + 4H]^{4+}$ (calcd): 733.64 (719.40), ($m/z$) for $[M + 5H]^{5+}$ (calcd): 564.52 (575.72). **8**: gradient, 15−40% MeCN in 6 min; yield, 66%; ESI-MS ($m/z$) for $[M + 3H]^{3+}$ (calcd): 619.02 (619.01). **9**: gradient, 10−50% MeCN in 6 min; yield, 46%; ESI-MS ($m/z$) for $[M + 3H]^{3+}$ (calcd): 1086.86 (1086.85), ($m/z$) for $[M + 4H]^{4+}$ (calcd): 815.39 (815.39). **10**: gradient, 0−40% MeCN in 6 min; yield, 65%; MALDI-MS ($m/z$) for $[M + H]^+$ (calcd): 1550.4 (1548.8). **11**: gradient, 0−40% MeCN in 6 min; yield, 64%; MALDI-MS ($m/z$) for $[M + H]^+$ (calcd): 1610.7 (1608.8). **12**: gradient, 0−40% MeCN in 6 min; yield, 56%; MALDI-MS ($m/z$) for $[M + H]^+$ (calcd): 1669.0 (1666.9). **13**: gradient, 0−40% MeCN in 6 min; yield, 69%; MALDI-MS ($m/z$) for $[M + H]^+$ (calcd): 1713.1 (1710.9). **14**: gradient, 10−40% MeCN in 6 min; yield, 57%; ESI-MS ($m/z$) for $[M + 2H]^{2+}$ (calcd): 899.97 (899.97), ($m/z$) for $[M + 3H]^{3+}$ (calcd): 600.32 (600.31). **15**: purification performed using a Kromasil C8 preparative column, gradient, 0−50% MeCN in 6 min; yield, 72%; ESI-MS ($m/z$) for $[M + 2H]^{2+}$ (calcd): 944.00 (944.00); ($m/z$) for $[M + 3H]^{3+}$ (calcd): 630.00 (629.66). **16**: purification performed using a Kromasil C8 preparative column, gradient, 0−50% MeCN in 6 min; yield, 64%; ESI-MS ($m/z$) for $[M + 2H]^{2+}$ (calcd): 1032.05 (1032.05), ($m/z$) for $[M + 3H]^{3+}$ (calcd): 688.70 (688.37). **17**: gradient, 0−50% MeOH in 6 min; yield, 40%; MALDI-MS ($m/z$) for $[M + H]^+$ (calcd): 3507.8 (3505.7). **18**: gradient, 0−50% MeOH in 6 min; yield, 70%; MALDI-MS ($m/z$) for $[M + H]^+$ (calcd): 3598.0 (3593.7). **19**: gradient, 0−50% MeOH in 6 min; yield, 74%; MALDI-MS ($m/z$) for $[M + H]^+$ (calcd): 3682.8 (3681.8). **20**: gradient, 0−50% MeOH in 6 min; yield, 75%; MALDI-MS ($m/z$) for $[M + H]^+$ (calcd): 3859.3 (3857.9). **21**: gradient, 10−65% MeCN in 6 min; yield, 79%; ESI-MS ($m/z$) for $[M + 2H]^{2+}$ (calcd): 1080.66 (1080.57), ($m/z$) for $[M + 3H]^{3+}$ (calcd): 721.05 (720.71). **22**: gradient, 10−40% MeCN in 6 min; yield, 42%; ESI-MS ($m/z$) for $[M + 2H]^{2+}$ (calcd): 1113.04 (1113.08), ($m/z$) for $[M + 3H]^{3+}$ (calcd): 742.73 (742.39).

**Synthesis of Fmoc−Lys(tris-*t*-Bu-DOTA)−OH (23).** To a solution of *N,N,N′,N′*-tetramethyl-*O*-(1*H*-benzotriazol-1-yl)uronium hexafluorophosphate (HBTU, 1.0 g, 2.65 mmol) and tris-*t*-Bu-DOTA (1.56 g, 2.72 mmol) in DMF (6 mL) was added diisopropylethylamine (DIPEA, 464 μL, 2.72 mmol). After 2 min reaction time, the mixture was added to a suspension of Fmoc−lysine (1.0 g, 2.72 mmol) in DMF (2 mL) and reacted for 30 min. Afterward, the nonreacted Fmoc−lysine was filtered off, and the solvent was removed. The crude product was purified by preparative HPLC using a gradient of 15−70% MeCN + 0.1% TFA over 10 min. The product was obtained as light yellow solid oil after lyophilization (815 mg, 883 μmol, 33%). $^1$H NMR (DMSO-$d_6$): δ 8.52 (bs, 1H), 7.91 (d, 2H, $J^3$ = 7.6), 7.75−7.72 (m, 2H), 7.69 (d, 1H, $J^3$ = 8.3), 7.43 (t, 2H, $J^3$ = 7.5), 7.33 (t, 2H, $J^3$ = 7.5), 4.33−4.20 (m, 2H), 3.96−3.90 (m, 2H), 3.61−2.87 (bm, 18H), 1.74−1.23 (m, 6H), 1.47 (s, 9H), 1.39 (s, 18H). $^{13}$C NMR (DMSO-$d_6$): δ 175.57, 173.86, 158.70, 158.35, 158.01, 156.11, 143.69, 140.65, 127.59, 126.30, 125.21, 120.08, 65.52, 54.56, 54.46, 53.54, 53.21, 53.19, 50.79, 50.69, 50.61, 46.57, 27.59, 23.07. ESI-MS ($m/z$) for $[M + Na]^+$ (calcd): 923.55 (923.54).

**Synthesis of $DOTA_{10}$−$Py5_{15}$−AngioPep−FP-T (24).** To a solution of $DOTA_{10}$−AngioPep−maleimide−FP-T conjugate (**9**, 3.1 mg, 0.95 μmol) and Py5 (0.7 mg, 1.90 μmol) in DMF (250 μL) was added DIPEA (0.32 μL, 1.90 μmol), and the mixture was reacted for 10 min. The crude product was purified by semipreparative HPLC using a gradient of 10−40% MeCN + 0.1% FA over 6 min. The product was obtained as a dark red solid after lyophilization (1.37 mg, 0.38 μmol, 40%). ESI-MS ($m/z$) for $[M + 2H]^{3+}$ (calcd): 1173.91 (1173.90), ($m/z$) for $[M + 3H]^{4+}$ (calcd): 880.68 (880.68).

**Synthesis of $PEG_3$−FP-T (25).** To a commercially available Rink Amide resin (50 μmol) were subsequently coupled Fmoc−$PEG_3$−OH and maleimido-hexanoic acid using standard amino acid coupling conditions. The product was cleaved from the resin as described before and purified by semipreparative HPLC using a gradient of 10−40% MeCN + 0.1% FA over 6 min. The product was obtained as colorless crystallizing oil after lyophilization (19 mg, 41.6 μmol, 83%). ESI-MS ($m/z$) for $[M + H]^+$ (calcd): 480.23 (480.23). Subsequently, a solution of this maleimide intermediate (4.8 mg, 10.5 μmol) in PB (phosphate buffer, 0.1 M, pH 4.0)/MeCN 1:1 (250 μL) was added to a solution of FP-T (**1**, 3.0 mg, 7.9 μmol), and the pH of the solution was adjusted to 7.0 using PB (0.5 M, pH 7.2, ∼ 50 μL). After 10 min, the product was purified by semipreparative HPLC using a gradient of 10−50% MeCN + 0.1% FA over 6 min. The product was isolated as colorless oil after lyophilization (2.72 mg, 3.26 μmol, 41%). ESI-MS ($m/z$) for $[M + H]^+$ (calcd): 836.45 (836.44).

**Synthesis of TfR-$P_s$−SiFA−$PEG_3$−Cysteine (26).** To a solution of TfR-$P_s$−SiFA−$PEG_3$−maleimide (**21a**, 6.2 mg, 3.48 μmol) in MeCN/PB (0.1M, pH 5.0) 1:1 (300 μL) was added a solution of cysteine (1.0 mg, 8.26 μmol) in $H_2O$ (100 μL), and the pH of the mixture was adjusted to 7.0 using PB (0.5 M, pH 7.2, ∼25 μL). After 5 min, the crude product was purified by semipreparative HPLC using a gradient of 10−65% MeCN + 0.1% FA over 6 min. The product was obtained as white solid after lyophilization (3.54 mg, 1.86 μmol, 53%). ESI-MS ($m/z$) for $[M + H]^+$ (calcd): 1903.96 (1902.96), ($m/z$) for $[M + 2H]^{2+}$ (calcd): 952.48 (951.98).

**Synthesis of Nonmodified Peptides TfR-$P_s$ (27), NTP (28), and $TAT_{49-57}$ (29).** The peptides were synthesized on solid support, deprotected, and cleaved using standard protocols as described before. The products were purified by semipreparative HPLC and isolated as white solids after lyophilization. Gradients used for HPLC purification, synthesis yields, and analytical data are given below.

**27**: gradient, 0−40% MeCN in 6 min; yield, 86%; ESI-MS ($m/z$) for $[M + H]^+$ (calcd): 892.47 (892.47). **28**: gradient, 0−30% MeCN in 6 min; yield, 73%; ESI-MS ($m/z$) for $[M + 2H]^{2+}$ (calcd): 642.39 (642.39). **29**: gradient, 0−30% MeCN in 6 min; yield, 71%; ESI-MS ($m/z$) for $[M + 4H]^{4+}$ (calcd): 335.72 (335.72); MALDI-MS ($m/z$) for $[M + H]^+$ (calcd): 1340.2 (1339.9).

**$^{18}$F Radiolabeling of 21.** Standard radiolabeling conditions: To a solution of dried $[n\text{-}Bu_4N]^{18}F$ complex (4.1−6.2 GBq) in DMSO (500 μL), obtained as described elsewhere,[61] was added a solution of **21** (25 nmol, 54 μg) in dry DMSO (2.5 μL), and the mixture was reacted for 5 min at ambient temperature without stirring. Subsequently, the reaction mixture was added to HEPES buffer (0.1 M, pH 4, 9 mL) and


dx.doi.org/10.1021/jm5004123 | J. Med. Chem. 2014, 57, 4368−4381

loaded on a Waters SepPak C-18 light cartridge, previously conditioned with ethanol (5 mL) and water (10 mL). The trapped product was washed with water (5 mL), eluted from the cartridge with ethanol (200 μL), and diluted with isotonic saline solution (2 mL). The purified product solution was subjected to analytical radio-HPLC, which showed an insufficient radiochemical purity of the product of 81−85%. Optimized radiolabeling conditions: Aqueous [$^{18}$F]fluoride in target water was passed through a SAX cartridge (Sep-Pak Accell Plus QMA Carbonate light (46 mg)) followed by 20 mL of air, 5 mL of anhydrous acetonitrile, and again 20 mL of air. The [$^{18}$F]fluoride was eluted with a solution of [$K^+$⊂K2.2.2]$OH^-$ in anhydrous acetonitrile (0.5 mL) containing 110 μmol Kryptofix 2.2.2 and 100 μmol KOH. To this solution were added first a solution of oxalic acid (1M, 21 μL) and subsequently a solution of **21** (25 nmol, 54 μg) in anhydrous DMSO (2.5 μL), and the mixture was reacted for 5 min at ambient temperature without stirring. Subsequently, the reaction mixture was added to HEPES buffer (0.1 M, pH 2, 9 mL) and loaded on a Waters SepPak C-18 light cartridge. The trapped product was washed with water (5 mL), eluted from the cartridge with ethanol (200 μL), and finally diluted with isotonic saline solution (2 mL). The purified product solution was subjected to analytical radio-HPLC. The radiolabeled product, [$^{18}$F]**21**, was found to be ≥98% pure and was obtained in specific activities of up to 80 GBq/μmol and radiochemical yields of up to 60% in a total synthesis time of 25 min.

**$^{68}$Ga Radiolabeling of 9, 17−20, 22, and 24.** A solution of the respective fusion molecule (10−12.5 nmol) in HEPES buffer (0.025 M, pH 4.0, 100 μL) was added to 170−290 MBq of $^{68}Ga^{3+}$ in sodium acetate solution obtained by fractioned elution of a $^{68}$Ge/$^{68}$Ga generator (IGG100, Eckert & Ziegler, Berlin, Germany) with HCl (0.1 M, 1.2 mL) and subsequent titration to pH 3.5−4.0 by addition of sodium acetate solution (1.25 M, 90−95 μL). After reaction for 10 min at 99 °C, the reaction mixtures were cooled to ambient temperature and analyzed by analytical radio-HPLC. The radiolabeled products, [$^{68}$Ga]**9**, [$^{68}$Ga]**17**−[$^{68}$Ga]**20**, and [$^{68}$Ga]**22** were found to be 96−98% pure and obtained in specific activities of 19.2−28.1 GBq/μmol.

## ■ ASSOCIATED CONTENT

### Ⓢ Supporting Information

Detailed description of the homology modeling of the $hD_2$ receptor; the model prediction, docking studies, molecular dynamics simulations, and results of these in silico studies; and a detailed description of the cytotoxicity and Calcein assays. This material is available free of charge via the Internet at http://pubs.acs.org.

### Accession Codes

PDB ID for protein $hD_3$ receptor in complex with antagonist eticlopride: 3PBL.

## ■ AUTHOR INFORMATION


### Corresponding Author

*Phone: +49 (0)621 383 3761; Fax: +49 (0)621 383 1910; E-mail: Carmen.Waengler@medma.uni-heidelberg.de.


### Notes

The authors declare no competing financial interest.

## ■ ACKNOWLEDGMENTS

C.W. thanks the Fonds der Chemischen Industrie for financial support. R.S. thanks the Natural Sciences and Engineering Council (NSERC) Canada and the FRSQ funded Quebec Bio-Imaging Network for financial support.

## ■ ABBREVIATIONS USED

BBB, blood−brain barrier; BC, (+)-butaclamol; Calcein-AM, calcein−acetoxymethylester complex; CNS, central nervous system; CP, chlorpromazine; DIPEA, *N*,*N*-diisopropylethylamine; DOTA, 1,4,7,10-tetraaza-cyclododecane-*N*,*N*′,*N*″,*N*‴-tetraacetic acid; DMF, *N*,*N*-dimethylformamide; DMFP, desmethoxy-fallypride; ESI, electrospray ionization; FP, fallypride; GPCR, G protein-coupled receptor; HBTU, *O*-(benzotriazol-1-yl)-*N*,*N*,*N*′,*N*′-tetramethyluronium hexafluorophosphate; HP, haloperidol; HPLC, high-performance liquid chromatography; KRB, Krebs ringer buffer; MALDI, matrix-assisted laser desorption/ionization; NIR, near-infrared; PEG, poly(ethylene glycol); PET, positron emission tomography; P-gp, P-glycoprotein; RP, raclopride; SIE, solvated interaction energy; SiFA, silicon fluoride acceptor; SPPS, solid-phase peptide synthesis; TfR, transferrin receptor; VIP, vasoactive intestinal peptide

## ■ REFERENCES


(1) Schirrmacher, R.; Bernard-Gauthier, V.; Reader, A.; Soucy, J. P.; Schirrmacher, E.; Wängler, B.; Wängler, C. Design of brain imaging agents for positron emission tomography: do large bioconjugates provide an opportunity for in vivo brain imaging? *Future Med. Chem.* **2013**, *5*, 1621−1634.

(2) Pardridge, W. M. Re-engineering biopharmaceuticals for delivery to brain with molecular trojan horses. *Bioconjugate Chem.* **2008**, *19*, 1327−1338.

(3) Pardridge, W. M. Drug transport across the blood-brain barrier. *J. Cereb. Blood Flow Metab.* **2012**, *32*, 1959−1972.

(4) Pardridge, W. M. Biopharmaceutical drug targeting to the brain. *J. Drug Targeting* **2010**, *18*, 157−167.

(5) Patel, M. M.; Goyal, B. R.; Bhadada, S. V.; Bhatt, J. S.; Amin, A. F. Getting into the brain: approaches to enhance brain drug delivery. *CNS Drugs* **2009**, *23*, 35−58.

(6) Smith, M. W.; Gumbleton, M. Endocytosis at the blood−brain barrier: from basic understanding to drug delivery strategies. *J. Drug Targeting* **2006**, *14*, 191−214.

(7) Pardridge, W. M. Blood−brain barrier delivery of protein and non-viral gene therapeutics with molecular trojan horses. *J. Controlled Release* **2007**, *122*, 345−348.

(8) Pardridge, W. M. Drug targeting to the brain. *Pharm. Res.* **2007**, *24*, 1733−1744.

(9) Gabathuler, R. Approaches to transport therapeutic drugs across the blood−brain barrier to treat brain diseases. *Neurobiol. Dis.* **2010**, *37*, 48−57.

(10) Lee, J. H.; Engler, J. A.; Collawn, J. F.; Moore, B. A. Receptor mediated uptake of peptides that bind the human transferrin receptor. *Eur. J. Biochem.* **2001**, *268*, 2004−2012.

(11) Boules, M.; Fredrickson, P.; Richelson, E. Bioactive analogs of neurotensin: focus on CNS effects. *Peptides* **2006**, *27*, 2523−2533.

(12) McGonigle, P. Peptide therapeutics for CNS indications. *Biochem. Pharmacol.* **2012**, *83*, 559−566.

(13) Cano, V.; Merino, B.; Ezquerra, L.; Somoza, B.; Ruiz-Gayo, M. A cholecystokinin-1 receptor agonist (CCK-8) mediates increased permeability of brain barriers to leptin. *Br. J. Pharmacol.* **2008**, *154*, 1009−1015.

(14) Kastin, A. J.; Akerstrom, V. Nonsaturable entry of neuropeptide Y into brain. *Am. J. Physiol.: Endocrinol. Metab.* **1999**, *276*, E479−E482.

(15) Chappa, A. K.; Audus, K. L.; Lunte, S. M. Characteristics of substance P transport across the blood−brain barrier. *Pharm. Res.* **2006**, *23*, 1201−1208.

(16) Thomas, F. C.; Taskar, K.; Rudraraju, V.; Goda, S.; Thorsheim, H. R.; Gaasch, J. A.; Mittapalli, R. K.; Palmieri, D.; Steeg, P. S.; Lockman, P. R.; Smith, Q. R. Uptake of ANG1005, a novel paclitaxel derivative, through the blood−brain barrier into brain and experimental brain metastases of breast cancer. *Pharm. Res.* **2009**, *26*, 2486−2494.

(17) Bertrand, Y.; Currie, J. C.; Demeule, M.; Regina, A.; Che, C.; Abulrob, A.; Fatehi, D.; Sartelet, H.; Gabathuler, R.; Castaigne, J. P.; Stanimirovic, D.; Beliveau, R. Transport characteristics of a novel

peptide platform for CNS therapeutics. *J. Cell. Mol. Med.* **2010**, *14*, 2827−2839.
(18) Che, C.; Yang, G. Q.; Thiot, C.; Lacoste, M. C.; Currie, J. C.; Demeule, M.; Regina, A.; Beliveau, R.; Castaigne, J. P. New angiopep-modified doxorubicin (ANG1007) and etoposide (ANG1009) chemotherapeutics with increased brain penetration. *J. Med. Chem.* **2010**, *53*, 2814−2824.
(19) Regina, A.; Demeule, M.; Che, C.; Lavallee, I.; Poirier, J.; Gabathuler, R.; Beliveau, R.; Castaigne, J. P. Antitumour activity of ANG1005, a conjugate between paclitaxel and the new brain delivery vector angiopep-2. *Br. J. Pharmacol.* **2008**, *155*, 185−197.
(20) Malcor, J. D.; Payrot, N.; David, M.; Faucon, A.; Abouzid, K.; Jacquot, G.; Floquet, N.; Debarbieux, F.; Rougon, G.; Martinez, J.; Khrestchatisky, M.; Vlieghe, P.; Lisowski, V. Chemical optimization of new ligands of the low-density lipoprotein receptor as potential vectors for central nervous system targeting. *J. Med. Chem.* **2012**, *55*, 2227−2241.
(21) Tian, X. H.; Wei, F.; Wang, T. X.; Wang, P.; Lin, X. N.; Wang, J.; Wang, D.; Ren, L. In vitro and in vivo studies on gelatin−siloxane nanoparticles conjugated with SynB peptide to increase drug delivery to the brain. *Int. J. Nanomed.* **2012**, *7*, 1031−41.
(22) Temsamani, J.; Bonnafous, C.; Rousselle, C.; Fraisse, Y.; Clair, P.; Granier, L. A.; Rees, A. R.; Kaczorek, M.; Scherrmann, J. M. Improved brain uptake and pharmacological activity profile of morphine-6-glucuronide using a peptide vector-mediated strategy. *J. Pharmacol. Exp. Ther.* **2005**, *313*, 712−719.
(23) Mazel, M.; Clair, P.; Rousselle, C.; Vidal, P.; Scherrmann, J. M.; Mathieu, D.; Temsamani, J. Doxorubicin−peptide conjugates overcome multidrug resistance. *Anticancer Drugs* **2001**, *12*, 107−16.
(24) Rousselle, C.; Clair, P.; Lefauconnier, J. M.; Kaczorek, M.; Scherrmann, J. M.; Temsamani, J. New advances in the transport of doxorubicin through the blood−brain barrier by a peptide vector-mediated strategy. *Mol. Pharmacol.* **2000**, *57*, 679−686.
(25) Dogrukol-Ak, D.; Banks, W. A.; Tuncel, N.; Tuncel, M. Passage of vasoactive intestinal peptide across the blood−brain barrier. *Peptides* **2003**, *24*, 437−444.
(26) Lindgren, M. E.; Hallbrink, M. M.; Elmquist, A. M.; Langel, U. Passage of cell-penetrating peptides across a human epithelial cell layer in vitro. *Biochem. J.* **2004**, *377*, 69−76.
(27) Qin, Y.; Chen, H. L.; Yuan, W. M.; Kuai, R.; Zhang, Q. Y.; Xie, F. L.; Zhang, L.; Zhang, Z. R.; Liu, J.; He, Q. Liposome formulated with TAT-modified cholesterol for enhancing the brain delivery. *Int. J. Pharm.* **2011**, *419*, 85−95.
(28) Qin, Y.; Chen, H. L.; Zhang, Q. Y.; Wang, X. X.; Yuan, W. M.; Kuai, R.; Tang, J.; Zhang, L.; Zhang, Z. R.; Zhang, Q.; Liu, J.; He, Q. Liposome formulated with TAT-modified cholesterol for improving brain delivery and therapeutic efficacy on brain glioma in animals. *Int. J. Pharm.* **2011**, *420*, 304−312.
(29) Rao, K. S.; Reddy, M. K.; Horning, J. L.; Labhasetwar, V. TAT-conjugated nanoparticles for the CNS delivery of anti-HIV drugs. *Biomaterials* **2008**, *29*, 4429−4438.
(30) Nam, Y. S.; Park, J. Y.; Han, S. H.; Chang, I. S. Intracellular drug delivery using poly(D,L-lactide-co-glycolide) nanoparticles derivatized with a peptide from a transcriptional activator protein of HIV-1. *Biotechnol. Lett.* **2002**, *24*, 2093−2098.
(31) Sharma, G.; Modgil, A.; Sun, C. W.; Singh, J. Grafting of cell-penetrating peptide to receptor-targeted liposomes improves their transfection efficiency and transport across blood−brain barrier model. *J. Pharm. Sci.* **2012**, *101*, 2468−2478.
(32) Meade, A. J.; Meloni, B. P.; Mastaglia, F. L.; Knuckey, N. W. The application of cell penetrating peptides for the delivery of neuroprotective peptides/proteins in experimental cerebral ischemia studies. *J. Exp. Stroke Transl. Med.* **2009**, *2*, 22−40.
(33) Malakotikhah, M.; Teixido, M.; Giralt, E. Toward an optimal blood−brain barrier shuttle by synthesis and evaluation of peptide libraries. *J. Med. Chem.* **2008**, *51*, 4881−4889.
(34) Swift, J. L.; Cramb, D. T. Nanoparticles as fluorescence labels: Is size all that matters? *Biophys. J.* **2008**, *95*, 865−876.
(35) Swift, J. L.; Heuff, R.; Cramb, D. T. A two-photon excitation fluorescence cross-correlation assay for a model ligand−receptor binding system using quantum dots. *Biophys. J.* **2006**, *90*, 1396−1410.
(36) Ceccarini, J.; Vrieze, E.; Koole, M.; Muylle, T.; Bormans, G.; Claes, S.; Van Laere, K. Optimized in vivo detection of dopamine release using F-18-fallypride PET. *J. Nucl. Med.* **2012**, *53*, 1565−1572.
(37) Rominger, A.; Cumming, P.; Xiong, G. M.; Koller, G.; Boning, G.; Wulff, M.; Zwergal, A.; Forster, S.; Reilhac, A.; Munk, O.; Soyka, M.; Wangler, B.; Bartenstein, P.; la Fougere, C.; Pogarell, O. [F-18]fallypride PET measurement of striatal and extrastriatal dopamine D-2/3 receptor availability in recently abstinent alcoholics. *Addict. Biol.* **2012**, *17*, 490−503.
(38) Kegeles, L. S.; Slifstein, M.; Xu, X. Y.; Urban, N.; Thompson, J. L.; Moadel, T.; Harkavy-Friedman, J. M.; Gil, R.; Laruelle, M.; Abi-Dargham, A. Striatal and extrastriatal dopamine D-2/D-3 receptors in schizophrenia evaluated with [F-18]fallypride positron emission tomography. *Biol. Psychiatry* **2010**, *68*, 634−641.
(39) Gao, M. Z.; Wang, M.; Mock, B. H.; Glick-Wilson, B. E.; Yoder, K. K.; Hutchins, G. D.; Zheng, Q. H. An improved synthesis of dopamine D-2/D-3 receptor radioligands [C-11]fallypride and [F-18]fallypride. *Appl. Radiat. Isot.* **2010**, *68*, 1079−1086.
(40) Majumdar, K. C.; Muhuri, S. Regioselective synthesis of pyrone-annulated sulfur heterocycles by aryl radical cyclization. *Synthesis* **2006**, 2725−2730.
(41) Majumdar, K. C.; Rafique-ul-Islam. Chemoselective synthesis of thieno [3,2-c] [1,8]naphthyridin-4(5H-ones by tandem cyclization. *Heteroat. Chem.* **2007**, *18*, 87−92.
(42) Liu, S. H.; Guo, Y. B.; Huang, R. Q.; Li, J. F.; Huang, S. X.; Kuang, Y. Y.; Han, L.; Jiang, C. Gene and doxorubicin co-delivery system for targeting therapy of glioma. *Biomaterials* **2012**, *33*, 4907−4916.
(43) Oh, S.; Kim, B. J.; Singh, N. P.; Lai, H.; Sasaki, T. Synthesis and anti-cancer activity of covalent conjugates of artemisinin and a transferrin-receptor targeting peptide. *Cancer Lett.* **2009**, *274*, 33−39.
(44) Demeule, M.; Currie, J. C.; Bertrand, Y.; Che, C.; Nguyen, T.; Regina, A.; Gabathuler, R.; Castaigne, J. P.; Beliveau, R. Involvement of the low-density lipoprotein receptor-related protein in the transcytosis of the brain delivery vector aAngiopep-2. *J. Neurochem.* **2008**, *106*, 1534−1544.
(45) Bertrand, Y.; Currie, J. C.; Poirier, J.; Demeule, M.; Abulrob, A.; Fatehi, D.; Stanimirovic, D.; Sartelet, H.; Castaigne, J. P.; Beliveau, R. Influence of glioma tumour microenvironment on the transport of ANG1005 via low-density lipoprotein receptor-related protein 1. *Br. J. Cancer* **2011**, *105*, 1697−1707.
(46) Kostikov, A. P.; Chin, J. S.; Orchowski, K.; Schirrmacher, E.; Niedermoser, S.; Jurkschat, K.; Iovkova-Berends, L.; Wängler, C.; Wängler, B.; Schirrmacher, R. Synthesis of [F-18]SiFB: a prosthetic group for direct protein radiolabeling for application in positron emission tomography. *Nat. Protoc.* **2012**, *7*, 1956−1963.
(47) Wängler, B.; Kostikov, A. P.; Niedermoser, S.; Chin, J. S.; Orchowski, K.; Schirrmacher, E.; Iovkova-Berends, L.; Jurkschat, K.; Wängler, C.; Schirrmacher, R. Protein labeling with the labeling precursor [F-18]SiFA-SH for positron emission tomography. *Nat. Protoc.* **2012**, *7*, 1964−1969.
(48) Wängler, C.; Niedermoser, S.; Chin, J. S.; Orchowski, K.; Schirrmacher, E.; Jurkschat, K.; Iovkova-Berends, L.; Kostikov, A. P.; Schirrmacher, R.; Wängler, B. One-step F-18-labeling of peptides for positron emission tomography imaging using the SiFA methodology. *Nat. Protoc.* **2012**, *7*, 1946−1955.
(49) Wetzl, B. K.; Yarmoluk, S. M.; Craig, D. B.; Wolfbeis, O. S. Chameleon labels for staining and quantifying proteins. *Angew. Chem., Int. Ed.* **2004**, *43*, 5400−5402.
(50) Iovkova, L.; Wängler, B.; Schirrmacher, E.; Schirrmacher, R.; Quandt, G.; Boening, G.; Schurmann, M.; Jurkschat, K. Para-functionalized aryl-di-tert-butylfluorosilanes as potential labeling synthons for F-18 radiopharmaceuticals. *Chem.—Eur. J.* **2009**, *15*, 2140−2147.
(51) Wängler, C.; Nada, D.; Hofner, G.; Maschauer, S.; Wängler, B.; Schneider, S.; Schirrmacher, E.; Wanner, K. T.; Schirrmacher, R.;

Prante, O. In vitro and initial in vivo evaluation of $^{68}$Ga-labeled transferrin receptor (TfR) binding peptides as potential carriers for enhanced drug transport into TfR expressing cells. *Mol. Imaging Biol.* **2011**, *13*, 332−341.
(52) Schirrmacher, E.; Wängler, B.; Cypryk, M.; Bradtmoller, G.; Schäfer, M.; Eisenhut, M.; Jurkschat, K.; Schirrmacher, R. Synthesis of p-(di-tert-butyl[(18)f]fluorosilyl)benzaldehyde ([F-18]SiFA-A) with high specific activity by isotopic exchange: A convenient labeling synthon for the F-18-labeling of n-amino-oxy derivatized peptides. *Bioconjugate Chem.* **2007**, *18*, 2085−2089.
(53) Wängler, C.; Waser, B.; Alke, A.; Iovkova, L.; Buchholz, H. G.; Niedermoser, S.; Jurkschat, K.; Fottner, C.; Bartenstein, P.; Schirrmacher, R.; Reubi, J. C.; Wester, H. J.; Wängler, B. One-step (18)F-labeling of carbohydrate-conjugated octreotate-derivatives containing a silicon-fluoride-acceptor (SiFA): in vitro and in vivo evaluation as tumor imaging agents for positron emission tomography (PET). *Bioconjugate Chem.* **2010**, *21*, 2289−2296.
(54) Wessmann, S. H.; Henriksen, G.; Wester, H. J. Cryptate mediated nucleophilic F-18-fluorination without azeotropic drying. *Nuklearmedizin* **2012**, *51*, 1−8.
(55) Niessen, K. V.; Höfner, G.; Wanner, K. T. Competitive MS binding assays for dopamine D-2 receptors employing spiperone as a native marker. *ChemBioChem* **2005**, *6*, 1769−1775.
(56) Bubik, M.; Ott, M.; Mahringer, A.; Fricker, G. Rapid assessment of p-glycoprotein-drug interactions at the blood-brain barrier. *Anal. Biochem.* **2006**, *358*, 51−58.
(57) Bauer, B.; Miller, D. S.; Fricker, G. Compound profiling for p-glycoprotein at the blood−brain barrier using a microplate screening system. *Pharm. Res.* **2003**, *20*, 1170−1176.
(58) Weksler, B.; Romero, I. A.; Couraud, P. O. The hCMEC/D3 cell line as a model of the human blood brain barrier. *Fluids Barriers CNS* **2013**, *10*, 16.
(59) Höfelschweiger, B. The Pyrylium Dyes: A New Class of Biolabels. Synthesis, Spectroscopy, and Application as Labels and in General Protein Assay, Ph.D. Thesis, University Regensburg, Regensburg, Germany, 2005.
(60) Wellings, D. A.; Atherton, E. Standard Fmoc protocols. *Methods Enzymol.* **1997**, *289*, 44−67.
(61) Iovkova-Berends, L.; Wangler, C.; Zoller, T.; Hofner, G.; Wanner, K. T.; Rensch, C.; Bartenstein, P.; Kostikov, A.; Schirrmacher, R.; Jurkschat, K.; Wangler, B. t-Bu(2)SiF-derivatized D(2)-receptor ligands: the first SiFA-containing small molecule radiotracers for target-specific PET-imaging. *Molecules* **2011**, *16*, 7458−7479.